EPJ manuscript No.
(will be inserted by the editor)

Interpretations of the new LHCb $P_c(4337)^+$ pentaquark state

Mao-Jun Yan[1], Fang-Zheng Peng[2], Mario Sánchez Sánchez[3], and Manuel Pavon Valderrama[2]

[1] CAS Key Laboratory of Theoretical Physics, Institute of Theoretical Physics, Chinese Academy of Sciences, Beijing 100190, China
[2] School of Physics, Beihang University, Beijing 100191, China
[3] Centre d'Études Nucléaires, CNRS/IN2P3, Université de Bordeaux, 33175 Gradignan, France

July 5, 2022

Abstract. Recently the LHCb collaboration has observed a new pentaquark state, the $P_c(4337)^+$. Owing to its proximity to the $\chi_{c0}(1S)p$, $\bar{D}^*\Lambda_c$, $\bar{D}\Sigma_c$ and $\bar{D}\Sigma_c^*$ thresholds, this new pentaquark might very well be a meson-baryon bound state. However its spin and parity have not been determined yet and none of the previous possibilities can be ruled out. We briefly explore a few of these options and the consequences they entail in the present manuscript: (i) the $P_c(4337)^+$ might be a $\chi_{c0}(1S)p$ bound state, (ii) the $P_c(4312)^+$ and $P_c(4337)^+$ might be $\bar{D}^*\Lambda_c$ and $\bar{D}\Sigma_c$ states close to threshold, respectively, where the Breit-Wigner mass might not correspond to the location of the poles, (iii) the locations of the $P_c(4312)^+$ and $P_c(4337)^+$ might be explained in terms of the $\bar{D}^*\Lambda_c$-$\bar{D}\Sigma_c$ and $\bar{D}^*\Lambda_c$-$\bar{D}\Sigma_c^*$ coupled channel dynamics. This last option, though not the most probable explanation, is still potentially compatible with the double peak solution of the $P_{cs}(4459)^0$ and with what we know of the $P_c(4312)^+$. As a byproduct of the previous explorations, we conjecture the existence of a series of anticharmed meson - antitriplet charmed baryon bound states and calculate their masses.

arXiv:2108.05306v2 [hep-ph] 4 Jul 2022

1 Introduction

The LHCb collaboration has announced [1] the observation of a new pentaquark in the $J/\psi p$ invariant mass distribution, where its mass and width are

$$M(P_c(4337)^+) = 4337^{+7+2}_{-4-2}\,\text{MeV}\,, \tag{1}$$

$$\Gamma(P_c(4337)^+) = 29^{+26+14}_{-12-14}\,\text{MeV}\,, \tag{2}$$

and the statistical significance of the signal varies between $3.1-3.7\,\sigma$ depending on the J^P assignment. This pentaquark, being relatively narrow, might be related to the already known $P_c(4312)^+$, $P_c(4440)^+$, $P_c(4457)^+$ [2] and $P_{cs}(4459)^0$ [3] (where from now on we will drop their charge superscript). Of course the question is what the nature of this state is: is it a compact pentaquark state or is it molecular? Does it have partners? Can it be grouped together with other known pentaquarks?

Here we will briefly review a few of the possibilities for explaining this new pentaquark (where we will concentrate on meson-baryon explanations) and the consequences that they entail. But before that, we comment on the fact that the $P_c(4312)$ is not observed in the new LHCb results [1], which is puzzling at first sight, but might be explained by the different production mechanisms ($\Lambda_b^0 \to J/\psi\, pK^-$ and $B_s^0 \to J\psi\, p\,\bar{p}$), though other explanations are also possible (e.g. poor statistics, they might be the same state, etc.). Thus for most of this manuscript we will assume that both the $P_c(4312)$ and $P_c(4337)$ exist and that they are different states. The possibilities we will explore are: (i) the $P_c(4337)$ is a hadrocharmonium, (ii) the actual masses of the $P_c(4312)$ and $P_c(4337)$ do not coincide with the experimental ones obtained from their Breit-Wigner parametrizations, and they are actually $\bar{D}^*\Lambda_c$ and $\bar{D}\Sigma_c$ molecular states, respectively, and (iii) the $P_c(4312)$ and $P_c(4337)$ are poles of the $\bar{D}^*\Lambda_c$-$\bar{D}\Sigma_c$ and $\bar{D}^*\Lambda_c$-$\bar{D}\Sigma_c^*$ coupled channel systems. This last option will be particularly interesting, though not for its power for explaining the $P_c(4337)$. Instead, it allows to deduce the probable existence of a series of anticharmed meson - antitriplet charmed baryon pentaquarks and to calculate their masses. It is worth mentioning that other works have also explored variations of the previous possibilities or new explanations: for instance, Ref. [4] has proposed that the $P_c(4312)$ and $P_c(4337)$ are simply two manifestations of the same state, while Ref. [5] suggests that the $P_c(4337)$ and $P_{cs}(4459)$ are actually part of the same hadrocharmonium octet.

Correspondence to: mpavon@buaa.edu.cn

2 Hadrocharmonium

A very straightforward explanation is that of a $\chi_{c0}(1S)p$ bound state [6–8], i.e. a hadrocharmonium state: the $\chi_{c0}p$ threshold is located merely 10 MeV above the $P_c(4337)$. The binding mechanism is a two-gluon exchange short-range force between the χ_{c0} and the proton, the strength of which is proportional to the chromopolarizability α_S of the charmonium. Chromopolarizabilities are in general not well known, but large-N_c estimations [7] indicate that it might very well be strong enough as to bind the $\chi_{c0}p$ and other charmonium - light baryon systems [8]. Besides, the now suspected existence of a $J/\psi J/\psi$ bound state [9], which depends on similar ingredients (binding mechanism, estimations of α_S, etc.) [10], if anything makes the hadrocharmonium explanation more believable. Though originally proposed to explain the $P_c(4312)$ [8], the uncertainties in

α_S are likely to be compatible with the $P_c(4337)$ being the $\chi_{c0}p$ hadrocharmonium (at least if binding energies are as dependent on α_S as in [7, 11]; in this regard we notice that Ref. [5] suggests an uncertainty of up to 100 MeV in the mass of the prospective $\chi_{c0}p$ bound state based on two different fits of α_S). This explanation will predict $J^P = \frac{1}{2}^+$ (which is incidentally the most favored J^P by the experimental data [1]) and a decay width of the order of the χ_{c0} charmonium width, i.e. about 10 MeV, to which we could add contributions from short-range $\chi_{c0}p \to \psi(1S, 2S)p$ P-wave operators. This could be consistent with the experimental decay width of the $P_c(4337)$ once we take into account the admittedly large uncertainties.

This explanation will also effectively decouple the $P_c(4337)$ from the other prospective charmed baryon - charmed antimeson molecular pentaquarks, as the $\chi_{c0}p \to \bar{D}^{(*)}\Sigma_c^{(*)}$ transitions are also P-wave and short-range (they involve the exchange of a charmed meson) and thus expected to be suppressed. If this happens to be the case, the current molecular descriptions of the $P_c(4312)$, $P_c(4440)$ and $P_c(4457)$ pentaquarks will be left unchanged. These descriptions are usually based on the lowest order, heavy-quark spin symmetric $\bar{D}^{(*)}\Sigma_c^{(*)}$ contact-range potential [12] and usually lead to the prediction of the same set of partners [13–19] (with a few differences if pion dynamics [20, 21] or the $\bar{D}\Lambda_{c1}(2595)$ channel [22–25] are included, while non-molecular schemes tend to predict a different set of partners [26, 27]; it is also worth noticing the possibility that only a subset of the previous three pentaquarks might be molecular [28]).

3 Shallow $\bar{D}^*\Lambda_c$ and $\bar{D}\Sigma_c$ states

A second, relatively prosaic explanation, involves not only the new $P_c(4337)$ pentaquark but also the previous $P_c(4312)$ as well, whose mass and width are [2]

$$M(P_c(4312)) = 4311.9 \pm 0.7^{+6.8}_{-0.6}\,\text{MeV}, \tag{3}$$

$$\Gamma(P_c(4312)) = 9.8 \pm 2.7^{+3.7}_{-4.5}\,\text{MeV}. \tag{4}$$

Here it is worth noticing that the difference in the masses of the $P_c(4312)$ and $P_c(4337)$ pentaquarks is

$$M(P_c(4337)) - M(P_c(4312))) \approx 25\,\text{MeV}\,, \tag{5}$$

which incidentally coincides with the mass difference between the $\bar{D}^*\Lambda_c$ and $\bar{D}\Sigma_c$ thresholds

$$M(\bar{D}\Sigma_c) - M(\bar{D}^*\Lambda_c) = 25.8\,\text{MeV}. \tag{6}$$

This is interesting, because if there are shallow $\bar{D}^*\Lambda_c$ and $\bar{D}\Sigma_c$ bound states, the Breit-Wigner parametrization used to determine their masses is likely to fail. For instance, the $Z_c(3900)$ and $Z_{cs}(3985)$ Breit-Wigner masses are above the $D^*\bar{D}$ and $D^*\bar{D}_s$-$D\bar{D}_s^*$ thresholds, yet theoretical analyses indicate that they might very well correspond with poles in $D^*\bar{D}$ and $D^*\bar{D}_s$-$D\bar{D}_s^*$ scattering below threshold [29, 30]. Regarding the $P_c(4312)$ the analysis of the JPAC collaboration already contemplated the possibility that it is a $\bar{D}\Sigma_c$ virtual state just below threshold, instead of the more common interpretation as a $\bar{D}\Sigma_c$ bound state at about 9 MeV below threshold [31]. We notice that the JPAC analysis [31] did not include the $\bar{D}^*\Lambda_c$ channel, which might alter their previous conclusions.

The most interesting consequence of this scenario would be the existence of $\bar{D}\Lambda_c$ and $\bar{D}^*\Lambda_c$ pentaquarks, which have indeed been theorized [32]. From a theoretical viewpoint their existence is precarious: in the one-boson-exchange (OBE) model the $\bar{D}^{(*)}$ and Λ_c can exchange two light-mesons, the sigma and the omega [1], where the contribution of the former is attractive and the later repulsive, leading to a potential of the type [32]

$$V_{\text{OBE}}(\bar{D}^*\Lambda_c) = \frac{g_{\omega 1}g_{\omega 2}}{4\pi}\,\frac{e^{-m_\omega r}}{r} - \frac{g_{\sigma 1}g_{\sigma 2}}{4\pi}\,\frac{e^{-m_\sigma r}}{r}\,, \tag{7}$$

where the indices $i = 1, 2$ refer to the charmed antimeson and charmed baryon, respectively, $g_{\omega i}$ and $g_{\sigma i}$ are the couplings to the omega and sigma, and $m_\omega = 780\,\text{MeV}$ and $m_\sigma \sim (400 - 600)\,\text{MeV}$ are the omega and sigma masses. Phenomenologically (vector meson dominance and linear sigma model) we expect $g_{\omega 1} = g_{\omega 2}/2 = m_V/(2f_\pi) \sim 2.9$ and $g_{\sigma 1} = g_{\sigma 2}/2 = \sqrt{2}\,m_N/(3f_\pi) \sim 3.4$, with m_V, m_N the vector meson and nucleon masses and $f_\pi = 130\,\text{MeV}$ the pion decay constant. The previous estimation of the couplings will give the upper hand to the attraction provided by the sigma meson ($g_{\sigma i} > g_{\omega i}$), potentially leading to bound states, as has been already proposed [32]. However, considering the approximate nature of the previous relations this is far from an established conclusion and the interaction could in principle be repulsive instead. In this regard, Ref. [33] also points out towards a possible $\bar{D}\Lambda_c$ bound state, while Refs. [34, 35] are less optimistic about this prospect. Thus determining whether one of the two $P_c(4312)$ and $P_c(4337)$ pentaquarks could correspond to a $\bar{D}^*\Lambda_c$ bound state will indeed have important consequences regarding the OBE model as applied to heavy hadrons.

From the effective field theory (EFT) perspective, the consequences of this scenario are also interesting. In EFT the charmed antimeson - charmed baryon interaction can be described with a non-relativistic potential that admits a low energy power-series expansion in terms of the ratio Q/M, where Q represents a low-energy scale (e.g. the pion mass or the momentum of the charmed hadrons) and M a high-energy scale (e.g. the rho mass or the momentum for which an external probe will be able to discern the internal structure of the charmed hadrons). Actually, in a theory with bound states (e.g. molecular pentaquarks) where pion exchanges and coupled channel effects are perturbative, the EFT potential at lowest or leading order (LO) takes the form of a momentum- and energy-independent contact-range potential

$$V_C(\vec{q}) = c\,, \tag{8}$$

with c a coupling constant representing the physics from the degrees of freedom not explicitly included in the EFT, e.g. scalar and vector meson exchanges, or from the high momentum modes of the degrees of freedom already included (i.e. renormalization, where we will elaborate later). This coupling can be further decomposed into different contributions depending on the quantum numbers and symmetries of the system. If

[1] The reason for discarding other light mesons is that the exchange of a pion is precluded by isospin symmetry and HQSS, while rho exchange is forbidden only by isospin.

we consider $\bar{D}^{(*)}\Lambda_c$, this is a particular instance of a charmed antimeson - antitriplet charmed baryon system, for which the potential reads

$$V_C(\bar{H}_c T_c) = \lambda^{(S)} d_a^{(S)} + \lambda^{(O)} d_a^{(O)} \,, \tag{9}$$

with $\bar{H}_c = \bar{D}$, $\bar{D}_s$ or $\bar{D}^*$, $\bar{D}_s^*$, $T_c = \Lambda_c$, Ξ_c, where we have expanded in terms of SU(3)-flavor representations, with $d_a^{(S)}$ and $d_a^{(O)}$ the singlet and octet couplings and $\lambda^{(S)}$ and $\lambda^{(O)}$ coefficients. We notice that there is no spin dependence as this is forbidden by heavy-quark spin symmetry (HQSS) (the reason being that the total light spin of the light diquark within the antitriplet baryons is zero).

If we particularize for the $\bar{D}^*\Lambda_c$ and the isoscalar $I = 0$ $\bar{D}^{(*)}\Xi_c$ systems, we find

$$V_C(\bar{D}^{(*)}\Lambda_c) = d_a^{(O)} = \tilde{d}_a \,, \tag{10}$$

$$V_C(\bar{D}^{(*)}\Xi_c, I = 0) = \frac{2}{3} d_a^{(S)} + \frac{1}{3} d_a^{(O)} = d_a \,, \tag{11}$$

where for notational convenience we have defined the couplings $\tilde{d}_a$ and d_a. The reason why we bring up the $\bar{D}^{(*)}\Xi_c$ system is the recent observation of the $P_{cs}(4459)$ pentaquark [3], the mass and width of which are

$$\begin{aligned} M_{P_{cs}} &= 4458.8 \pm 2.9^{+4.7}_{-1.1}\,\text{MeV} \,, \\ \Gamma_{P_{cs}} &= 17.3 \pm 6.5^{+8.0}_{-5.7}\,\text{MeV} \,, \end{aligned} \tag{12}$$

where its most usual molecular interpretation is that of a $\bar{D}^*\Xi_c$ bound state with $I = 0$ [36–39], an interpretation further supported by previous predictions of $\bar{D}^*\Xi_c$ states [40, 41] with similar masses (and widths in the case of [40]). This system depends on the d_a coupling defined above, which should be attractive and strong enough as to bind the system if the $P_{cs}(4459)$ is indeed a molecular state. Now, if the $P_c(4312)$ and $P_c(4337)$ were to be $\bar{D}^*\Lambda_c$ and $\bar{D}\Sigma_c$ shallow bound or virtual states, this will in turn imply an attractive $\tilde{d}_a$ coupling (though probably not as strong as d_a). From SU(3)-flavor symmetry the interaction of the other S-wave $\bar{H}_c T_c$ systems can be expressed in terms of $\tilde{d}_a$ and d_a

$$V_C(\bar{D}_s^{(*)}\Lambda_c) = \frac{1}{2}(d_a + \tilde{d}_a) \,, \tag{13}$$

$$V_C(\bar{D}^{(*)}\Xi_c, I = 1) = \tilde{d}_a \,, \tag{14}$$

$$V_C(\bar{D}_s^{(*)}\Xi_c) = \tilde{d}_a \,. \tag{15}$$

Provided that the $\bar{D}^*\Lambda_c$ and $I = 0$ $\bar{D}\Xi_c^*$ bind or are close to binding, this will imply that all the previous systems are also attractive enough as to generate bound or virtual states near threshold, which will be possible to detect in the $J/\psi\,\Lambda$, $J/\psi\,\Sigma$ and $J/\psi\,\Xi$ channels.

4 $\bar{D}^*\Lambda_c$-$\bar{D}\Sigma_c$ and $\bar{D}^*\Lambda_c$-$\bar{D}\Sigma_c^*$ states

We now consider the third interpretation, namely that the $P_c(4312)$ and $P_c(4337)$ are poles within the $\bar{D}^*\Lambda_c$-$\bar{D}\Sigma_c$ and $\bar{D}^*\Lambda_c$-$\bar{D}\Sigma_c^*$ coupled channel dynamics. This idea, though interesting, will fail to provide a unified description of the $P_c(4312)$ and $P_c(4337)$ pentaquarks, at least within the uncertainties of the EFT we will be using. What we will get instead is the prediction of a $\bar{D}\Sigma_c^*$ pentaquark in the vicinity of 4370 MeV, in agreement with previous theoretical works [13, 16–19].

From a theoretical perspective the previous coupled channel dynamics are really interesting, as they raise the question of how to incorporate them within the EFT formalism. This is done by proposing a *power counting*, i.e. a principle by which to order the EFT contributions to the meson-baryon potential from more to less relevant at low energies. In this case the EFT description will require more elaboration than the single channel contact-range potential we discussed in the previous section. Before presenting this description in detail, we provide a brief overview of a few relevant EFT ideas in the following lines.

The interpretation of pentaquark states as shallow meson-baryon bound states allows the application of the EFT formalism. The reason is that the molecular picture implicitly assumes the existence of a separation of scales, as this description only makes sense when the size of a pentaquark as a bound system is larger than the size of its components. EFTs are constructed by writing down all possible interactions involving the low energy degrees of freedom of the theory (in our case charmed hadrons and pions) that are compatible with the known low energy symmetries (most notably HQSS, flavor and chiral symmetries). In principle this generates an infinite number of interactions and couplings, though not all them are equally important. Indeed, EFT interactions can be ordered from more to less relevant at low energies by means of a power counting, a criterion by which to decide what is the size of a given coupling.

It is important to emphasize that power counting is not uniquely determined within a given EFT, but instead depends on choices regarding the expected size of several physical effects. Owing to a scarcity of experimental data that can directly constrain the meson-baryon interactions, the determination of the power counting will rely on a series of assumptions. At this point two warnings are worth mentioning: the first is that changing these assumptions changes the counting. The second is that even for systems for which experimental data are abundant, such as the two-nucleon system, completely reasonable power counting expectations have been subverted upon closer theoretical examination, a very well-known example being how the KSW counting [42, 43] was discovered not to generate a convergent EFT expansion [44].

In this manuscript we will explore power counting in a constructive manner: first, we state a series of assumptions and the consequences they entail, including what type of pentaquark spectrum they predict. Then, we will revisit the assumptions and refine them, leading to modifications of the power counting and new predictions. We will end up with three power countings (*A*, *B* and *C*). In this section we deal with the first of these countings, *A*, which we determine by following these steps:

a) We begin by discussing the general properties of the EFT describing a two-hadron bound state, including the counting of the contact-range potential and the pions (if present).
b) We apply the previous ideas to determine the counting of the single channel $\bar{D}^*\Lambda_c$ and $\bar{D}\Sigma_c^{(*)}$ systems at low energies.
c) Then we consider the role of the $\bar{D}^*\Lambda_c$-$\bar{D}\Sigma_c$ and $\bar{D}^*\Lambda_c$-$\bar{D}\Sigma_c^*$ coupled channel dynamics, which contains a contact-range and pion exchange piece. We argue that the contact-range

piece survives at leading order, while pion exchanges are subleading.

This last choice is what defines counting A. Later in Sect. 6 we will revisit the assumptions about coupled channel dynamics made in the present section and propose other two countings, B and C. However, for the set of choices explored in this manuscript, we consistently reproduce the narrow $P_c(4380)$ predicted in previous works [13, 16–19] instead of the $P_c(4337)$.

4.1 General considerations

We first consider the general features of the lowest order EFT description of a two-hadron system with a low-lying bound state, which we will then particularize to the molecular pentaquarks relevant to this work. From the EFT point of view the soft scale Q will be given by the momenta of the hadrons p and the pion mass m_π, to which we will add the bound state momentum $\gamma_2 = \sqrt{2\mu B_2}$, with μ the reduced mass of the system and B_2 its binding energy. The hard scale M will be given by the vector meson mass m_ρ or by the typical momentum scale at which the internal structure of the hadrons becomes apparent. Contributions to the potential will be categorized as Q^ν (shorthand for $(Q/M)^\nu$), that is, by their power scaling with respect to the soft scale Q.

From counting powers of Q and M directly, the lowest order EFT potential possible is given by

$$V^{(0)}(\vec{q}) = V_C(\vec{q}) + V_{\rm OPE}(\vec{q})\,, \tag{16}$$

with V_C a momentum- and energy-independent contact-range potential and $V_{\rm OPE}$ the one pion exchange (OPE) potential, which we write as

$$V_{\rm OPE}(\vec{q}) = -\frac{12\pi}{\mu\,\Lambda_{\rm OPE}}\,\vec{T}_1\cdot\vec{T}_2\,\frac{\vec{S}_{L1}\cdot\vec{q}\,\vec{S}_{L2}\cdot\vec{q}}{\vec{q}^2+m_\pi^2}\,, \tag{17}$$

where $\vec{T}_i$ and $\vec{S}_{Li}$ are the isospin and light-spin operators of hadrons $i = 1, 2$, μ the reduced mass of the system and $\Lambda_{\rm OPE}$ the characteristic OPE scale. If we count $\Lambda_{\rm OPE}$ as a hard scale, the OPE potential is of order Q^0 and so is the complete lowest order potential. Yet, it happens that the actual counting of the lowest order potential can differ from this estimation.

The first obvious modification to the power counting happens in systems with bound states. This comes from the observation that the existence of bound states requires the resummation of a potential V, a condition which in terms of power counting can be written as follows

$$O(V) = O(VG_0V)\,, \tag{18}$$

where $G_0 = 1/(E_2 - H_0)$ is the resolvent operator (E_2 is the center-of-mass energy of the two-body system and H_0 its kinetic energy operator), which scales as Q ($\sim\gamma_2$) when integrated in a loop:

$$\int_\Lambda \frac{d^3\vec{q}}{(2\pi)^3}\,\frac{1}{E_2-\frac{q^2}{2\mu}} = \frac{\mu}{2\pi}\left(\gamma_2+\Lambda\beta(\frac{\gamma_2}{\Lambda})\right), \tag{19}$$

where Λ represents a cutoff (the loop integral is linearly divergent and hence requires regularization), $\gamma_2 = \sqrt{-2\mu E_2}$ with μ the reduced mass of the two-body system and $\beta(x)$ a function that depends on our choice of a regulator. From this, the potential has to be counted as $V\sim Q^{-1}$ for it to be able to generate a bound state.

When confronting this conclusion with the order Q^0 EFT potential, it is apparent that either the contact- or the finite-range piece has to be promoted to Q^{-1}. A well-known counting argument states that for a two-body system with a shallow bound state, the contact-range coupling will scale as [45]

$$c^{(R)} \sim \frac{2\pi}{\mu\sqrt{2\mu B_2}} \sim O\left(\frac{1}{Q}\right), \tag{20}$$

where B_2 refers to the binding energy of the system and the superscript $^{(R)}$ indicates that we are dealing with the *renormalized* coupling (*loosely speaking*, the part of the coupling that does not depend on the cutoff). This estimation comes from equating V_C and $V_CG_0V_C$ to make them comply with the power counting requirements for a bound state and taking only the finite part of the loop integration of G_0 in Eq. (19).

For the counting of the finite-range piece we first decompose the spin structure of the OPE potential in a spin-spin and tensor component

$$V_{\rm OPE}(\vec{q}) = -\frac{4\pi}{\mu\,\Lambda_{\rm OPE}}\,\vec{T}_1\cdot\vec{T}_2\Big[\frac{\vec{S}_{L1}\cdot\vec{S}_{L2}\,\vec{q}^2}{\vec{q}^2+m_\pi^2} + \frac{3\,\vec{S}_{L1}\cdot\vec{q}\,\vec{S}_{L2}\cdot\vec{q}-\vec{S}_{L1}\cdot\vec{S}_{L2}\,\vec{q}^2}{\vec{q}^2+m_\pi^2}\Big], \tag{21}$$

which is but a reordering of Eq. (17). The tensor component requires S- to D-wave transitions and we will assume it to be kinematically suppressed. Thus, it will not be considered further as part of our calculations. The spin-spin component acts on S-waves and its counting can be determined from the calculation of the following ratio

$$\frac{\langle V_S G_0 V_S\rangle}{\langle V_S\rangle} = \frac{Q}{\Lambda_S} = TS\,\frac{m_\pi}{\Lambda_{\rm OPE}}\,f(\frac{k}{m_\pi})\,, \tag{22}$$

where V_S refers to the spin-spin component of OPE, the matrix elements are taken for S-wave scattering states of center-of-mass momentum k and $f(x) = 1 - 13/6x^2 + O(x^4)$ is a function determining the momentum dependence of this ratio; its Taylor expansion is taken from [46] and its usually decreases with x (meaning that spin-spin OPE becomes more perturbative at higher momenta), i.e. we can take $f(k/m_\pi) = 1$ without loss of generality. The first line of Eq. (22) is just the generic scaling of iterated spin-spin OPE when no assumptions are made about the size of V_S, which is encoded in the spin-spin scale Λ_S. The second line is the result of the concrete calculation of the ratio of the iteration of the potential over the potential, where $\Lambda_{\rm OPE}$ is the OPE scale as we defined it in Eq. (17) and S, T are simply $\vec{T}_1\cdot\vec{T}_2$ and $\vec{S}_{L1}\cdot\vec{S}_{L2}$, respectively. From a direct comparison between the two lines, the characteristic momentum scale associated with spin-spin OPE is

$$\Lambda_S = \frac{1}{TS}\Lambda_{\rm OPE}\,. \tag{23}$$

Depending on its concrete evaluation we will be able to decide whether spin-spin OPE is Q^0 or Q^{-1} within EFT.

4.2 The $\bar{D}^*\Lambda_c$, $\bar{D}\Sigma_c$ and $\bar{D}\Sigma_c^*$ diagonal potential

The application of the previous ideas to the $\bar{D}^*\Lambda_c$, $\bar{D}\Sigma_c$ and $\bar{D}\Sigma_c^*$ systems is straightforward. If we assume that these three systems bind or are close to binding, the LO potential is of order Q^{-1} and only contains a contact-range interaction

$$V^{(-1)}(\vec{q}, \bar{D}^*\Lambda_c) = V_C(\bar{D}^*\Lambda_c) = \tilde{d}_a\,, \tag{24}$$
$$V^{(-1)}(\vec{q}, \bar{D}\Sigma_c^{(*)}) = V_C(\bar{D}\Sigma_c^{(*)}) = c_a\,. \tag{25}$$

OPE does not contribute though, as neither of these three systems can exchange one pion (two pions will be the minimum): OPE is forbidden by isospin symmetry in the $\bar{D}^*\Lambda_c$ system (and more generally by HQSS in the $\bar{H}_c T_c$ systems), while for $\bar{D}\Sigma_c$ and $\bar{D}\Sigma_c^*$ the $\bar{D}$ is a pseudoscalar and cannot emit or absorb a pion (unless it turns into a $\bar{D}^*$, but in this case we will have a coupled channel effect).

4.3 Counting of the $\bar{D}^*\Lambda_c$-$\bar{D}\Sigma_c$ and $\bar{D}^*\Lambda_c$-$\bar{D}\Sigma_c^*$ dynamics

As previously mentioned, the $\bar{D}^*\Lambda_c$ and $\bar{D}\Sigma_c$ thresholds are merely 25 MeV away from each other. This suggests that coupled channel dynamics could be important in this and other similar cases.

For a two-body system with a shallow bound state, we naively expect coupled channel effects to be suppressed (or enhanced, depending on the case) by a factor of B_2/Δ_{CC}, with B_2 and Δ_{CC} the bound state energy and the mass gap between the two channels. Alternatively, in the EFT language, we will compare the characteristic momentum scales of the bound state and the mass gap, $Q \sim \gamma_2 = \sqrt{2\mu B_2}$ and $M \sim \Lambda_{CC} = \sqrt{2\mu\Delta_{CC}}$, respectively, with μ the reduced mass of the two-body system [47].

If we consider the usual, single-channel molecular interpretation of the $P_c(4312)$ pentaquark — a $\bar{D}\Sigma_c$ bound state about 9 MeV below threshold – the EFT expansion parameter is expected to be the ratio of the two-body binding momentum (or the pion mass) over the rho meson mass

$$\frac{Q}{M} \sim \frac{\max(m_\pi, \gamma_2)}{m_\rho} \sim 0.18\,, \tag{26}$$

where $\gamma_2 = \sqrt{2\mu B_2} \sim 137$ MeV (which coincides with the pion mass) is the binding momentum, with μ the reduced mass of the $\bar{D}\Sigma_c$ or $\bar{D}^*\Lambda_c$ system, and $m_\rho \simeq 770$ MeV the rho meson mass. In this case the binding energy is comparable to the 25 MeV mass gap between the $\bar{D}^*\Lambda_c$ and $\bar{D}\Sigma_c$ thresholds, yielding

$$\left(\frac{\gamma_2}{\Lambda_{CC}}\right)^2 \sim \frac{B_2}{\Delta_{CC}} \sim 0.35 \quad \text{for } \bar{D}^*\Lambda_c\text{-}\bar{D}\Sigma_c\,. \tag{27}$$

This ratio, though not particularly large, happens to be larger than the expansion parameter for the $P_c(4312)$ as a single channel bound state. From this, it is apparent that this particular coupled channel effect enters between LO and NLO (i.e. next-to-leading-order). Thus we will simply include the $\bar{D}^*\Lambda_c$-$\bar{D}\Sigma_c$ coupled channel dynamics in the LO of the theory.

Naturally, if we consider the $\bar{D}^*\Lambda_c$-$\bar{D}\Sigma_c$ transition potential in the $J = \frac{1}{2}$ configuration, we might consider the $J = \frac{3}{2}$ $\bar{D}^*\Lambda_c$-$\bar{D}\Sigma_c^*$ coupled channel dynamics as well. The $\bar{D}^*\Lambda_c$-$\bar{D}\Sigma_c^*$ combination offers two possible interpretations of the $P_c(4337)$ pentaquark:

(i) The $P_c(4337)$ as a lower mass pole in the $\bar{D}^*\Lambda_c$-$\bar{D}\Sigma_c^*$ coupled channel dynamics, with the higher mass pole corresponding to the predicted narrow $P_c(4380)$ $\bar{D}\Sigma_c^*$ state [13, 16–18] (where [18] claims evidence of its existence within the original data of Ref. [2]).

(ii) The $P_c(4337)$ as the higher mass pole, which implies that this pentaquark is indeed the previously mentioned narrow $\bar{D}\Sigma_c^*$ bound state and that its binding energy has been underestimated.

Actually, if we only use momentum- and energy-independent contact-range interactions, interpretation (i) can be discarded: with this type of contact-range interaction a pole originally located below $\bar{D}^*\Lambda_c$ can only become a resonance above this threshold if it hits a second pole further below the $\bar{D}^*\Lambda_c$ threshold first, where this type of trajectory is nicely illustrated in Ref. [48]. That is, the LO potential requires the lower mass pole to be below the $\bar{D}^*\Lambda_c$ threshold, which is incompatible with the assumptions in (i). Thus, unless we include energy or momentum dependent contact-range interactions explicitly [2], this leaves us with interpretation (ii), which actually might help explain one feature of the $P_c(4337)$: its large width. In fact, if the $P_c(4337)$ corresponds to a $\bar{D}\Sigma_c^*$ molecule, the width of the Σ_c^* will have to be added to the intrinsic width of the $P_c(4337)$ as a pole of the $\bar{D}^*\Lambda_c$-$\bar{D}\Sigma_c^*$ coupled channel dynamics. It is worth noticing though that the width of a bound Σ_c^* will be narrower than that of a free Σ_c^*, because of the reduction of phase space for the pion owing to binding effects.

Independently of the interpretation, the estimations for the convergence parameter of the EFT expansion for the $P_c(4337)$ as a $\bar{D}\Sigma_c$ molecule and the size of the coupled channel dynam-

[2] Here we might be tempted to consider the addition of S-to-D-wave interactions (contact-range or pions). The rationale is that for L-wave interactions with $L \geq 1$, when the strength of the interaction weakens, the trajectory of poles is such that a bound state becomes a resonance (instead of a virtual state as happens in S-waves), check Ref. [48]. It is not clear whether this strategy will work though. If a non-perturbative S-to-D-wave interaction generates a shallow bound state below threshold, and this state is mostly S-wave, at low energies the naive expectation is that it is possible to describe it in EFT terms with an effective S-wave contact-range interaction. Thus, its trajectory in the complex plane is naively expected to be that of an S-wave pole, i.e. to bounce back at threshold and become a virtual state. Yet, this is an interesting possibility that deserves further investigation in the future.

ics are

$$\frac{Q}{M} \sim \frac{\sqrt{2\mu|E_2|}}{m_\rho} \sim 0.42 - 0.44\,, \tag{28}$$

$$\left(\frac{\gamma_2}{\Lambda_{CC}}\right)^2 \sim \frac{|E_2|}{\Delta_{CC}} \sim 0.54 - 0.62 \quad \text{for } \bar{D}^*\Lambda_c\text{-}\bar{D}\Sigma_c^*\,, \tag{29}$$

where E_2 refers to the center-of-mass energy of the resonance with respect to either of the thresholds. That is, the EFT expansion for the $P_c(4337)$ is not expected to work as well as in the $P_c(4312)$, which will have to be taken into account when assessing whether these two resonances can be described coherently within the same formalism.

At this point it is interesting to notice that the previous coupled channel dynamics are analogous to what might be happening with the $P_{cs}(4459)$ [38]. The most prosaic molecular explanation of the $P_{cs}(4459)$ pentaquark is that of a $\bar{D}^*\Xi_c$ bound state with $J = \frac{1}{2}$ or $\frac{3}{2}$. Yet, the $\bar{D}\Xi_c'$ and $\bar{D}\Xi_c^*$ channels are actually pretty close too, just about 30 MeV below and above the $\bar{D}^*\Xi_c$ threshold. Repeating the previous arguments we find

$$\frac{Q}{M} \sim \frac{\sqrt{2\mu|B_2|}}{m_\rho} \sim 0.27\,, \tag{30}$$

$$\left(\frac{\gamma_2}{\Lambda_{CC}}\right)^2 \sim \frac{|B_2|}{\Delta_{CC}} \sim 0.54 - 0.60 \quad \text{for } \bar{D}\Xi_c\text{-}\bar{D}^*\Xi_c \text{ and } \bar{D}^*\Xi_c\text{-}\bar{D}\Xi_c^*\,. \tag{31}$$

This prompted us to include this type of coupled channel dynamics, which breaks the spin degeneracy of the $P_{cs}(4459)$, in a previous work [38]. Besides, the experimental analysis of Ref. [3] actually proposes two possible interpretations for the $P_{cs}(4459)$: a single peak interpretation, which yields the mass and width that we previously referred to in Eq. (12) or a double peak interpretation in which the $P_{cs}(4459)$ is actually composed of the following two states

$$M(P_{cs1}) = 4454.9 \pm 2.7\,\text{MeV}\,, \tag{32}$$
$$\Gamma(P_{cs1}) = 7.5 \pm 9.7\,\text{MeV}\,, \tag{33}$$

$$M(P_{cs2}) = 4467.8 \pm 3.7\,\text{MeV}\,, \tag{34}$$
$$\Gamma(P_{cs2}) = 5.3 \pm 5.3\,\text{MeV}\,, \tag{35}$$

which we call P_{cs1} and P_{cs2}. The $\bar{D}\Xi_c'$-$\bar{D}^*\Xi_c$ and $\bar{D}^*\Xi_c$-$\bar{D}\Xi_c^*$ coupled channel dynamics is able to explain this double peak pattern provided that the P_{cs1} and P_{cs2} are $J = \frac{3}{2}$ and $\frac{1}{2}$ states, respectively. From now on (unless stated otherwise), we will use the two peak solution found by the LHCb experimental analysis [3], i.e. we will assume the existence of the previous two P_{cs} peaks.

4.4 The $\bar{D}^*\Lambda_c$-$\bar{D}\Sigma_c$ and $\bar{D}^*\Lambda_c$-$\bar{D}\Sigma_c^*$ transition potential

The description of the previous coupled channel transitions depends on the choice of a LO EFT potential. In line with the expected enhancement of contact-range interactions when there are bound states, we assume that they are included in the LO potential. OPE also contributes to the $\bar{D}^*\Lambda_c$-$\bar{D}\Sigma_c$ and $\bar{D}^*\Lambda_c$-$\bar{D}\Sigma_c^*$ transitions, but its effects will be subleading (we elaborate in a few lines). From the previous, we end up with the LO EFT potential:

$$V_C(\bar{H}_c T_c - \bar{H}_c S_c) = \lambda^{(O)}\, e_b^{(O)} \vec{\sigma}_{L1} \cdot \vec{\epsilon}_{L2}\,, \tag{36}$$

where $S_c = \Sigma_c$, Ξ_c', Ω_c or Σ_c^*, Ξ_c^*, Ω_c^* are the sextet charmed baryons, $e_b^{(O)}$ is a coupling (which only involves the octet components of the $\bar{H}_c T_c$ and $\bar{H}_c S_c$ systems, hence the $^{(O)}$ superscript), $\lambda^{(O)}$ a numerical flavor factor, $\vec{\sigma}_{L1}$ the light-spin operator for the light-quark within the charmed mesons and $\vec{\epsilon}_{L2}$ the polarization vector for the light-diquark within the sextet baryons. By particularizing for the $J = \frac{1}{2}$ $\bar{D}^*\Lambda_c$-$\bar{D}\Sigma_c$ and $J = \frac{3}{2}$ $\bar{D}^*\Lambda_c$-$\bar{D}\Sigma_c^*$ channels, the potentials happen to be identical and given by

$$V_C(P_c^N, J = \tfrac{1}{2}, \tfrac{3}{2}) = \begin{pmatrix} d_a^{(O)} & -e_b^{(O)} \\ -e_b^{(O)} & c_a^{(O)} \end{pmatrix}, \tag{37}$$

$$= \begin{pmatrix} \tilde{d}_a & -\sqrt{3}\, e_b \\ -\sqrt{3}\, e_b & c_a \end{pmatrix}, \tag{38}$$

where in the second line we have redefined the couplings as to use the same notation as for the $\bar{D}^*\Lambda_c$ case, see Eq.(10). For the $J = \frac{1}{2}$ $\bar{D}\Xi_c'$-$\bar{D}^*\Xi_c$ and $J = \frac{3}{2}$ $\bar{D}^*\Xi_c$-$\bar{D}\Xi_c^*$ systems we have instead

$$V_C(P_{cs}, J = \tfrac{1}{2}) = \begin{pmatrix} c_a^{(O)} & \frac{e_b^{(O)}}{\sqrt{3}} \\ \frac{e_b^{(O)}}{\sqrt{3}} & \frac{2}{3} d_a^{(S)} + \frac{1}{3} d_a^{(O)} \end{pmatrix} \tag{39}$$

$$= \begin{pmatrix} c_a & e_b \\ e_b & d_a \end{pmatrix}, \tag{40}$$

$$V_C(P_{cs}, J = \tfrac{3}{2}) = \begin{pmatrix} \frac{2}{3} d_a^{(S)} + \frac{1}{3} d_a^{(O)} & \frac{e_b^{(O)}}{\sqrt{3}} \\ \frac{e_b^{(O)}}{\sqrt{3}} & c_a^{(0)} \end{pmatrix} \tag{41}$$

$$= \begin{pmatrix} d_a & e_b \\ e_b & c_a \end{pmatrix}, \tag{42}$$

where, again, we write the potential both in terms of its SU(3) flavor representations and the couplings we already defined in Ref. [38].

Regarding the OPE potential, the particular $\bar{H}_c T_c$-$\bar{H}_c S_c$ transition in which it is strongest is $\bar{D}^{(*)}\Lambda_c$-$\bar{D}^{(*)}\Sigma_c^{(*)}$, for which it reads [3]

$$V_{\text{OPE}}(\vec{q}, \bar{D}^{(*)}\Lambda_c \to \bar{D}^{(*)}\Sigma_c^{(*)}) = -\frac{g_1 g_3}{\sqrt{2} f_\pi^2}\, \vec{\tau}_1 \cdot \vec{\imath}_2\, \frac{\vec{\sigma}_{L1} \cdot \vec{q}\, \vec{\epsilon}_{L2} \cdot \vec{q}}{\vec{q}^{\,2} + m_\pi^2}\,, \tag{43}$$

where g_1 is the axial coupling of the pion to the charmed mesons (for which we have $g_1 = 0.59 \pm 0.01 \pm 0.07$ [49, 50] from the strong D^* decays, or the values extracted from the updated D^*

[3] For the other $\bar{H}_c T_c$-$\bar{H}_c S_c$ transitions, their OPE, one-kaon and one-eta exchange potentials can be derived from the $\bar{D}^{(*)}\Lambda_c$-$\bar{D}^{(*)}\Sigma_c^{(*)}$ one and the relevant SU(3)-flavor symmetry relations.

decay widths [51], leading to the estimations $g_1 = 0.54$ [52] or $g_1 = 0.56 \pm 0.01$ [53]), $|g_3| = 0.973^{+0.019}_{-0.042}$ [54] the axial coupling for the $\Lambda_c \to \Sigma_c^{(*)}$ transition in the convention by Cho [55] (which is related to the convention by Yan [56] by the relation $g_3^{(\mathrm{Cho})} = -\sqrt{3} g_2^{(\mathrm{Yan})}$; we notice that Ref. [54] originally uses the Yan convention), $f_\pi = 130\,\mathrm{MeV}$ the pion weak decay constant and $m_\pi = 138\,\mathrm{MeV}$ the pion mass. The $\vec{\tau}_1$ and $\vec{t}_2$ isospin operators are formally analogous to the $\vec{\sigma}_{L1}$ and $\vec{\epsilon}_{L2}$ light spin operators, and their evaluation yields $|\vec{\tau}_1 \cdot \vec{t}_2| = \sqrt{3}$ and 0 for $I = \frac{1}{2}$ and $\frac{3}{2}$, respectively.

For counting the OPE potential, we rewrite it in the form proposed in Eq. (21)

$$V_{\mathrm{OPE}}(\vec{q}, \bar{D}^{(*)}\Lambda_c \to \bar{D}^{(*)}\Sigma_c^{(*)}) = -\frac{4\pi}{\mu\,\Lambda_{\mathrm{OPE}}}\,\vec{\tau}_1 \cdot \vec{t}_2\,\frac{\vec{\sigma}_{L1} \cdot \vec{\epsilon}_{L2}\,\vec{q}^{\,2}}{\vec{q}^{\,2} + m_\pi^2} + \dots\,, \tag{44}$$

where the dots indicate the tensor forces, which we ignore (as they involve D-waves). From this we find $\Lambda_{\mathrm{OPE}} = 1610\,\mathrm{MeV}$, which implies a spin-spin OPE scale of $\Lambda_S = 537\,\mathrm{MeV}$ for $\bar{D}^{(*)}\Lambda_c \to \bar{D}^{(*)}\Sigma_c^{(*)}$ (where $T = \vec{\tau}_1 \cdot \vec{t}_2 = \sqrt{3}$ and $S = \vec{\sigma}_{L1} \cdot \vec{\epsilon}_{L2} = \sqrt{3}$). Combined with the coupled channel suppression, the relative size of OPE with respect to the LO diagonal contact-range interaction happens to be

$$\frac{Q}{\Lambda_S}\left(\frac{\gamma_2}{\Lambda_{CC}}\right)^2 \sim 0.09\,,\ 0.14 - 0.16 \quad \text{for } \bar{D}^*\Lambda_c\text{-}\bar{D}\Sigma_c,\ \bar{D}^*\Lambda_c\text{-}\bar{D}\Sigma_c^*. \tag{45}$$

This indicates that spin-spin OPE is NLO or smaller. This type of demotion of the OPE potential is compatible with what happens in the charmed meson-antimeson [47] and charmed baryon-antibaryon systems [57].

At this point it is interesting to compare with [19], a work which previously considered the dynamics of the $\bar{D}^{(*)}\Lambda_c \to \bar{D}^{(*)}\Sigma_c^{(*)}$ transitions. The most important difference with our approach is that Ref. [19] iterates OPE (both spin-spin and tensor) to all orders. This requires the inclusion of the S-to-D-wave contacts for the numerical renormalization of the amplitudes. The reason is that tensor OPE happens to be a singular power-law potential, diverging as $1/r^3$ at distances smaller than the Compton wave length of the pion [58]. For hard enough cut-offs this divergence is probed, requiring the inclusion of new contact-range couplings for its proper renormalization. That is, the pentaquark description of Ref. [19] significantly differs from ours in what regards to the structure of the contact-range potential, where the specific reason why we have less couplings is the assumption that tensor OPE is perturbative (as spin-spin OPE is known not to modify the power counting of the contacts when iterated [59]).

Unfortunately, Ref. [19] does not explore the question of whether tensor OPE is perturbative or not: this will require re-expanding the amplitudes in powers of V_{OPE}, which is tedious, and then comparing this reexpanded amplitude with the original one in which OPE is fully iterated. However, the fact that the S-to-D-wave contacts are enough to numerically renormalize the amplitudes in [19] points towards the hypothesis that they are perturbative. The evidence is circumstantial though and comes from a comparison with a previous result regarding the non-perturbative renormalization of OPE in the two-nucleon system [60], where a tensor contact-range structure (which generates the aforementioned S-to-D-wave contacts) was tried, but failed to renormalize OPE in all partial waves. The reason why the tensor contact-range structure fails is the particular way in which singular potentials are renormalized in coupled channels [61, 62], yet these results do not preclude the possibility that a tensor contact-range potential might work in specific cases. Be it as it may, the techniques developed in the two-nucleon sector to renormalize tensor OPE both perturbatively [44] and non-perturbatively [60–63] could be applied to the case of molecular pentaquarks in the future to solve this issue.

4.5 Description of the $P_c(4337)$

We will now calibrate the LO potential as to reproduce the properties of the $P_c(4312)$, $P_c(4337)$ and the two P_{cs} peaks. First, a few remarks:

a) The masses and widths of the $P_c(4312)$ and $P_c(4337)$ depend mostly on c_a and e_b, respectively, while $\tilde{d}_a$ impacts mostly the width of the $P_c(4312)$ (because of the effect of the final $\bar{D}^*\Lambda_c$ interaction on the partial decay width into this channel).

b) Conversely, the masses and widths of the $J = \frac{1}{2}$ P_{cs2} depend on d_a and e_b, respectively. However this does not represent the full width of the P_{cs1} and P_{cs2} pentaquarks: it only takes into account the $\bar{D}\Xi_c'$ decay channel for $J = \frac{1}{2}$, which only contributes $(1-2)\,\mathrm{MeV}$ to its width according to Ref. [38], while the $J = \frac{3}{2}$ state is predicted to be stable. From this and the phenomenological calculation of Ref. [40], which indicates that the $J/\psi\Lambda$ partial decay width is also small, we expect the main decay channel of the two P_{cs} to be $\bar{D}_s^*\Lambda_c$.

With the experimental information available and the assumptions we are making here, we will be able to determine all the four couplings.

Regarding the widths, we will assume that for molecular pentaquarks they are saturated by the charmed antimeson - charmed baryon decay channels, with only a small fraction of the width coming from decays into charmonium and a light baryon. This is compatible with the branching ratio limits determined by GlueX [64], which are

$$\mathcal{B}(P_c(4312) \to J/\psi p) < 4.6\%\,, \tag{46}$$

at the 90% confidence level. For simplicity we will generally ignore the decays involving pions: concrete calculations [65] show that this type of partial decay width is very similar in size to the (narrow) decay width of the charmed baryon within the molecular pentaquark. Thus, the pion decays will only be important for molecular pentaquarks containing a Σ_c^* charmed baryon.

With the ingredients we have included within our EFT, the only pentaquark for which we can confidently calculate the width is the $P_c(4312)$: if assumed to be a $\bar{D}\Sigma_c$ bound state, according to the arguments in the previous paragraph, its width should be saturated by the $\bar{D}^*\Lambda_c$ decay channel (the decay into

$\bar{D}\Lambda_c$ is forbidden by HQSS). For the two P_{cs} pentaquarks, we already mentioned that the main decay channel is expected to be $\bar{D}_s^*\Lambda_c$ instead. Finally, for the $P_c(4337)$ the situation is a bit more subtle than in the previous examples: on the one hand, if it contains a Σ_c^*, this will provide a contribution to the width that does not directly appear in our EFT calculations, which should instead predict a narrower $P_c(4337)$. On the other, the momenta involved in the prospective $P_c(4337)$ decays are larger and not necessarily ideal for a LO description in terms of momentum-independent contact-range interactions. That is, if the $P_c(4337)$ were to really be a $\bar{D}\Sigma_c^*$ molecule, its description would probably require the inclusion of NLO contributions if we are to achieve a similar theoretical accuracy as for the $P_c(4312)$.

From the previous considerations, we will determine c_a, d_a, $\tilde{d}_a$ and e_b from

a) the mass and width of the $P_c(4312)$ (as we expect the decay width to be saturated by $\bar{D}^*\Lambda_c$),
b) the masses of the P_{cs1} and P_{cs2} pentaquark.

We advance that the determination of the couplings is not unique and there are two types of solutions, one in which the $\bar{D}^*\Lambda_c$ diagonal interaction is attractive and another in which it is repulsive; we will choose the attractive solution, as it is better aligned with phenomenological expectations about its sign (see the discussion around Eqs. (53-56)). For obtaining results we will renormalize the LO potential by including a Gaussian regulator, a cutoff and making the coupling dependent on the cutoff:

$$\langle p'|V_C|p\rangle = c(\Lambda)\, g(\frac{p'}{\Lambda})\, g(\frac{p}{\Lambda})\,, \tag{47}$$

with Λ the cutoff and $g(x) = e^{-x^2}$ the regulator function. For the cutoff we will take a central value of $\Lambda = 0.75\,\text{GeV}$, i.e. of the order of the rho meson mass, which we will vary in the $(0.5 - 1.0)\,\text{GeV}$ window for estimating uncertainties.

For convenience we will express c_a, d_a, $\tilde{d}_a$ and e_b relative to a reference value, namely the c_a^{ref} coupling that reproduces the mass of the $P_c(4312)$ as a single-channel $\bar{D}\Sigma_c$ state

$$c_a^{\text{ref}}(\Lambda) = -1.19\,(-(2.17 - 0.80))\,\text{fm}^2\,, \tag{48}$$

where the values in parentheses correspond to the (0.5−1.0) GeV cutoff variation. With this we find:

$$c_a = +1.25\,(1.41 - 1.18)\,c_a^{\text{ref}}\,, \tag{49}$$
$$\tilde{d}_a = +1.32\,(1.40 - 1.26)\,c_a^{\text{ref}}\,, \tag{50}$$
$$d_a = +1.07\,(1.13 - 1.04)\,c_a^{\text{ref}}\,, \tag{51}$$
$$e_b = \pm 0.28\,(0.41 - 0.21)\,c_a^{\text{ref}}\,, \tag{52}$$

which we will call "set A" and merits a few comments: (i) a plus sign indicates an attractive interaction (the reference coupling is attractive), (ii) for reproducing the mass of the $P_c(4312)$, in the coupled channel case c_a has to be more attractive than in the single channel case to compensate for the repulsion generated by e_b, (iii) the change in c_a after the inclusion of the coupled channels (~ 0.25) is compatible with the 0.35 estimation we made for the relative size of this effect, see Eq. (27), (iv) as in Eq. (48), the number outside the parentheses are the $\Lambda = 0.75\,\text{GeV}$ results, while the first and second number inside the parentheses represent the $\Lambda = 0.5$ and $1.0\,\text{GeV}$ results, respectively.

We find it surprising that $\tilde{d}_a$ turns out to be so attractive, which is worth a more extended comment. First, as already mentioned, there are actually two possible solutions for the previous determination of the couplings: one in which $\tilde{d}_a$ is attractive and another one in which it is repulsive. However, here we have discarded the repulsive solution because it will turn out to be incompatible with the width of the P_{cs} pentaquarks once we include the $\bar{D}_s^*\Lambda_c$ channel, as will be explained later. Second, from phenomenological arguments we expect the following

$$\text{(a)}\quad c_a, d_a, \tilde{d}_a < 0\,, \tag{53}$$
$$\text{(b)}\quad c_a \sim d_a\,, \tag{54}$$
$$\text{(c)}\quad |c_a|, |d_a| > |\tilde{d}_a|\,, \tag{55}$$
$$\text{(d)}\quad |c_a|, |d_a|, |\tilde{d}_a| \gg |e_b|\,. \tag{56}$$

Condition (a) is derived from the observation that the combination of scalar and vector meson exchange is expected to be attractive for c_a, d_a and $\tilde{d}_a$, though the case for an attractive $\tilde{d}_a$ is weaker than for c_a, d_a, see discussion around Eq. (7). Condition (b) is a consequence of light-meson exchanges, which should have similar strengths in both cases, a point that seems to be confirmed in the EFT description of the P_{cs} [38]. Condition (c) comes from the observation that vector meson exchange is repulsive for $\bar{D}^*\Lambda_c$ (while scalar meson exchange is always attractive). Condition (d) reflects that e_b has its origins in the magnetic-like coupling of the vector mesons to the heavy hadrons, which generates a spin-spin component of the potential that is expected to be weaker than its central components [38, 66, 67]. In this regard, it is interesting to notice that phenomenological studies of molecular pentaquarks that ignore these spin-spin interactions do in general a good job in explaining or even predicting the spectrum [14, 40]. These conditions can be used as *priors* on the basis of which to consider a particular determination of the couplings as being more or less likely. In particular, Eqs. (49-52) fulfill (a), (b), (d), but not (c), which is the reason why we commented that $\tilde{d}_a$ is surprisingly attractive. Yet, $\tilde{d}_a$ is probably the coupling for which our determination should be less reliable.

With these couplings, we predict two bound $\bar{D}^*\Lambda_c$ pentaquarks and the expected $\bar{D}\Sigma_c^*$ pentaquark

$$M(\bar{D}^*\Lambda_c, \tfrac{1}{2}) = 4246.6\,(4250.1 - 4244.6)\,\text{MeV}\,, \tag{57}$$
$$M(\bar{D}^*\Lambda_c, \tfrac{3}{2}) = 4257.1\,(4261.1 - 4255.0)\,\text{MeV}\,, \tag{58}$$

$$M(\bar{D}\Sigma_c^*, \tfrac{3}{2}) = 4371.2\,(4370.7 - 4371.3) - i\,5.3(4.2 - 5.5)\,\text{MeV}. \tag{59}$$

While the mass of the $\bar{D}\Sigma_c^*$ pentaquark is definitely heavier than the experimental one, thus reducing the likelihood of the $\bar{D}\Sigma_c^*$ interpretation of the $P_c(4337)$, we nonetheless notice that if we add the 15 MeV width of the Σ_c^* to the prediction of the $\bar{D}\Sigma_c^*$ pentaquark, we will end up with about 25 MeV, coinciding with the experimental central value.

However the previous does not take into account a very important difference between the $J = \frac{1}{2}$ and $\frac{3}{2}$ channels: if the

$J = \frac{3}{2}$ configuration can indeed be identified with the $P_c(4337)$, the EFT expansion is expected to converge slowly, as shown in Eqs. (28) and (29). That is, a coherent description of the $P_c(4312)$ and $P_c(4337)$ pentaquarks will benefit from the inclusion of subleading order effects. Right now, this is not feasible owing to the increase in the number of parameters that this entails: the combined EFT description of the $P_c(4312)$ and $P_c(4337)$ contains a total of 6 parameters at NLO: the three LO couplings — c_a, e_b and $\tilde{d}_a$ — and the three couplings corresponding to the Q^2 derivative version of the LO potential. In addition, the one pion exchange (OPE) potential is also expected to enter at NLO. We find it worth noticing that not all the Q^2 contact-range interactions enter at NLO: for instance, there is a tensor coupling between the S-wave $\bar{D}^*\Lambda_c$ and the D-wave $\bar{D}\Sigma_c$ and $\bar{D}\Sigma_c^*$ channels, plus a quadrupolar E2-like tensor coupling between the S- and D-waves of the $\bar{D}\Sigma_c^*$ channel. These interactions are however only promoted one order with respect to their naive dimensional estimation and hence enter at N^{2}LO. We refer to Appendix A for a detailed explanation of how we count these subleading contact-range interactions.

As the inclusion of NLO operators is not a viable strategy at the moment, this brings us to a different consistency check: use two different c_a's for the $P_c(4312)$ and $P_c(4337)$ and check whether their values are consistent within the estimated expansion parameters in Eqs. (28) and (29). The motivation is that if the power counting of these two molecular candidates is not the same or it does not converge at the same rate, the couplings are not necessarily identical if we force the same power counting. If we perform this exercise with the previously obtained values of d_a, $\tilde{d}_a$ and e_b, we get

$$\begin{aligned} c_a(P_c') &= 1.81\,(2.26 - 1.59)\, c_a^{\rm ref} \\ &= 1.45\,(1.61 - 1.36)\, c_a(P_c)\,, \end{aligned} \tag{60}$$

that is, the values of the two couplings differ again by a magnitude that could be compatible with the unaccounted subleading order corrections for the $P_c(4337)$, which we estimated to have a relative size of $Q/M \simeq 0.42 - 0.44$, see Eq. (28). In this case the two $\bar{D}^*\Lambda_c$-$\bar{D}\Sigma_c^*$ poles are at

$$M(\bar{D}^*\Lambda_c, \tfrac{3}{2}) = 4250.4\,(4255.3 - 4247.5)\,\text{MeV}\,, \tag{61}$$

$$M(\bar{D}\Sigma_c^*) = 4337.0 - i\,8.0\,(6.7 - 8.7)\,\text{MeV}\,, \tag{62}$$

where the width of the $P_c(4337)$ is predicted to be 16 MeV, which would be compatible with the experimental value once we add the Σ_c^* width. From this point of view, the previous failure to accurately reproduce the $P_c(4337)$ pentaquark as a $\bar{D}\Sigma_c^*$ bound state would merely reflect the uncertainty of the LO calculation we are doing here. But still, the previous conclusion requires that the $P_c(4337)$ is a $\bar{D}\Sigma_c^*$ molecule in the first place (otherwise the expansion parameter will be smaller, making it impossible to argue for $c_a(P_c)$ and $c_a(P_c')$ to be compatible), which merely show that this hypothesis is self-consistent at LO. This potential compatibility between the $P_c(4312)$ and $P_c(4337)$ could be disproved at NLO, where the relative difference between $c_a(P_c)$ and $c_a(P_c')$ shrinks to $(Q/M)^2 \simeq 0.18 - 0.19$. Yet, there is circumstantial evidence from other calculations [19, 21] that subleading corrections are unlikely to make the descriptions of the $P_c(4312)$ and $P_c(4337)$ consistent with each other. Had we used the EFT expansion parameters derived from the $P_c(4312)$ instead, the conclusion would have been different: the $P_c(4337)$ would have been inconsistent with the $\bar{D}\Sigma_c^*$ molecular interpretation both at the level of the theoretical and experimental uncertainties already at LO, as in this case the expansion parameter is $Q/M \sim 0.18$, see Eq. (26).

Indeed, this underlines the importance of correctly assessing the uncertainties of the LO calculations for the prospective $\bar{D}\Sigma_c^*$ pentaquark. In this regard, in [68], which includes error estimations, the mass of the $\bar{D}\Sigma_c^*$ state is calculated to be $4375.5^{+13.7}_{-23.3}$ MeV for a cutoff $\Lambda = 1.0$ GeV and assuming that the $P_c(4440)$ and $P_c(4457)$ are $J = \frac{3}{2}$ and $\frac{1}{2}$ $\bar{D}^*\Sigma_c$ molecules, respectively. That is, the calculations of Ref. [68] might be compatible within errors with the $P_c(4337)$ being a $\bar{D}\Sigma_c^*$ state, though close to the $2\,\sigma$ level (i.e. a difference of 39 MeV between the central value of this theoretical prediction and the mass of the $P_c(4337)$, which is to be compared with an error of 23 MeV). More recently, Ref. [19] includes the $\bar{D}^{(*)}\Lambda_c$ channels, tensor OPE and a series of S-to-D-wave contact-range couplings required to numerically renormalize the amplitudes (but not the momentum dependent correction of the c_a coupling), yet it still predicts the $\bar{D}\Sigma_c^*$ molecule at 4376 MeV. Other calculation that is worth noticing is Ref. [21], which does not include the $\bar{D}^{(*)}\Lambda_c$ channel explicitly but implicitly as intermediate states in the leading two-pion exchange (TPE) potential. This effect, which will be subleading order in our counting (though enhanced with respect to naive estimations owing to the smaller energy denominators in the TPE diagrams with $\Sigma_c^{(*)} \to \Lambda_c$ transitions), generates a $\bar{D}\Sigma_c^*$ potential that is more attractive than the $\bar{D}\Sigma_c$ one, and predicts the mass of the $\bar{D}\Sigma_c^*$ pentaquark to be about 4362 MeV, i.e. $10 - 20$ MeV lighter than the predictions in theories with contact-interactions and with/without OPE (e.g. the pionful EFT of Ref. [15] estimates the mass of the $\bar{D}\Sigma_c^*$ to be close to 4380 MeV). These and other subleading effects could be worth considering in the future.

All things considered, the error of the LO calculation seems to be neither large enough as to easily include the location of the $P_c(4337)$ nor small enough as to completely exclude it (a NLO calculation would easily solve the issue, though). Here, if besides the cutoff uncertainty we also include the uncertainties coming (i) from the experimental input, (ii) from HQSS violations (which would imply that the couplings we have calculated from one state might be off up to a factor of $\Lambda_{\rm QCD}/m_Q \sim 0.15$ in the charm sector, with $\Lambda_{\rm QCD} \approx 200$ MeV) and (iii) from the intrinsic EFT uncertainty (i.e. Q/M, for which we will take the larger 0.27 estimation for the $P_{cs}(4459)$ in Eq. (30) instead of the smaller 0.18 for the $P_c(4312)$ in Eq. (26)), we will arrive at

$$M(\bar{D}\Sigma_c^*) = 4371.4^{+15.4}_{-17.6} - i\,5.1^{+2.8}_{-4.1}\,\text{MeV}\,, \tag{63}$$

which is compatible (within theoretical uncertainties) with the aforementioned calculations of Refs. [15, 21, 68], but not with the mass of the $P_c(4337)$ (except, again, at the 2σ level, and yet only for a pessimistic estimation of Q/M [4]). If this estimation of the errors is to be considered reliable enough, it will be improbable that the $P_c(4337)$ is actually a $\bar{D}\Sigma_c^*$ molecule. On a different line of thought, if the predicted $P_c(4380)$ [13, 16–19] is experimentally confirmed, the molecular interpretation of the

[4] The more conservative choice $Q/M \sim 0.18$ would have yielded $M(\bar{D}\Sigma_c^*) = 4371.4^{+13.2}_{-13.0} - i\,5.1^{+2.4}_{-3.4}$ MeV instead, leading to a discrepancy above the 2.5σ level.

$P_c(4337)$ as a $\bar{D}\Sigma_c^*$ will also be excluded (unless it is a different and unusual experimental manifestation of the $P_c(4380)$).

5 New molecular pentaquarks with antitriplet charmed baryons

It is interesting to notice that the couplings in set A (i.e. Eqs. (49-52)) will lead to the existence of a series of $\bar{H}_c T_c$ bound states. This can be deduced from the values of the couplings and the single channel potentials in Eqs. (13-15), leading to the (single channel) predictions

$$M(\bar{D}_s\Lambda_c) = 4236.1\,(4236.6 - 4236.3)\,\text{MeV}\,, \quad (64)$$
$$M(\bar{D}_s^*\Lambda_c) = 4378.1\,(4379.4 - 4377.6)\,\text{MeV}\,, \quad (65)$$

$$M(\bar{D}\Xi_c(0)) = 4324.2\,(4323.6 - 4325.1)\,\text{MeV}\,, \quad (66)$$

$$M(\bar{D}\Xi_c(1)) = 4310.4\,(4313.0 - 4309.4)\,\text{MeV}\,, \quad (67)$$
$$M(\bar{D}^*\Xi_c(1)) = 4449.4\,(4453.0 - 4447.4)\,\text{MeV}\,, \quad (68)$$

$$M(\bar{D}_s\Xi_c) = 4409.9\,(4413.2 - 4408.1)\text{MeV}\,, \quad (69)$$
$$M(\bar{D}_s^*\Xi_c) = 4551.5\,(4555.8 - 4548.8)\,\text{MeV}\,, \quad (70)$$

where for the $\bar{D}^{(*)}\Xi_c$ configurations the value in parentheses represents the isospin ($I = 0, 1$) and, as usual, the central value corresponds to $\Lambda = 0.75\,\text{GeV}$ and the values in parentheses to $\Lambda = (0.5 - 1.0)\,\text{GeV}$. However, there are a few instances of nearby $\bar{H}_c T_c$ and $\bar{H}_c S_c$ thresholds, as shown in Fig. 1, a fact that points towards the importance of coupled channel dynamics. As a consequence, a consistent prediction of the masses of these states requires the analysis of the power counting of the different coupled channel effects relevant to each of these molecules, as we have already done for the $P_c(4312)$ in Eq. (27).

This is done in Table 1 , from which we can appreciate the existence of a few coupled channel effects that are worth considering. For instance, the description of the $J = \frac{1}{2}$ $\bar{D}_s^*\Lambda_c$ system will be improved by the addition of the $\bar{D}\Xi_c'$ channel, leading to the combined $\bar{D}_s^*\Lambda_c$-$\bar{D}\Xi_c'$ potential

$$V_C(\tilde{P}^{\Lambda}_{cs}, J = \frac{1}{2}) = \begin{pmatrix} \frac{1}{2}\,(d_a + \tilde{d}_a) - \sqrt{2}\,e_b \\ -\sqrt{2}\,e_b \quad c_a \end{pmatrix}. \quad (71)$$

Yet, the most clear examples of the importance of coupled channel effects happen in the $\bar{D}^*\Xi_c(I = 1)$ and $\bar{D}_s^*\Xi_c$ molecules, which are really close to a series of nearby channels:

a) For the $I = 1$, $S = -1$ and $J = \frac{1}{2}$ $\bar{D}^*\Xi_c(I = 1)$ system, we will consider the $\bar{D}_s\Sigma_c$-$\bar{D}\Xi_c'(1)$-$\bar{D}^*\Xi_c(1)$ basis in which the potential reads

$$V_C(P^{\Sigma}_{cs}, J = \frac{1}{2}) = \begin{pmatrix} \frac{2}{3}\,c_a & -\frac{\sqrt{2}}{3}\,c_a & \sqrt{2}\,e_b \\ -\frac{\sqrt{2}}{3}\,c_a & \frac{1}{3}\,c_a & -e_b \\ \sqrt{2}\,e_b & -e_b & \tilde{d}_a \end{pmatrix}. \quad (72)$$

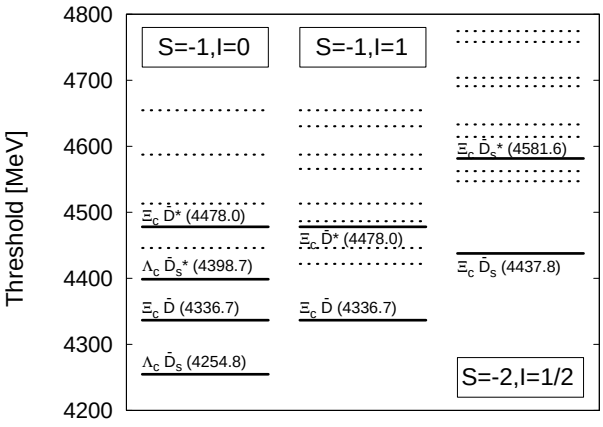


Fig. 1. Masses of the $\bar{H}_c T_c$ and $\bar{H}_c S_c$ meson-baryon thresholds in the strangeness $S = -1$ and -2 sectors. The thresholds containing an antitriplet charmed baryon are marked using solid lines and include a label indicating the explicit meson-baryon system under consideration and its mass in MeV. The dotted lines indicate the thresholds containing a sextet charmed baryon, but no label is provided to avoid overcluttering the figure: in the $S = -1$, $I = 0$ sector, the dotted lines correspond to the $\bar{D}\Xi_c'$, $\bar{D}\Xi_c^*$, $\bar{D}^*\Xi_c'$ and $\bar{D}^*\Xi_c^*$ thresholds (ordered according to increasing mass); in the $S = -1$, $I = 1$ sector to the $\bar{D}_s\Sigma_c$, $\bar{D}\Xi_c'$, $\bar{D}_s\Sigma_c^*$, $\bar{D}\Xi_c^*$, $\bar{D}_s^*\Sigma_c$, $\bar{D}^*\Xi_c'$, $\bar{D}_s^*\Sigma_c^*$ and $\bar{D}^*\Xi_c^*$ thresholds; finally, for the $S = -2$, $I = \frac{1}{2}$ sector we have $\bar{D}_s\Xi_c'$, $\bar{D}\Omega_c$, $\bar{D}_s\Xi_c^*$, $\bar{D}\Omega_c^*$, $\bar{D}_s^*\Xi_c'$, $\bar{D}^*\Omega_c$, $\bar{D}_s^*\Xi_c^*$ and $\bar{D}^*\Omega_c^*$, respectively. Naively, the relative importance of nearby coupled channels is expected to scale as B_2/Δ_{CC}, with B_2 the two-body binding energy and Δ_{CC} the mass gap between thresholds, check Eqs. (27), (29) and (31) for concrete examples.

b) For the the $I = 1$, $S = -1$ and $J = \frac{3}{2}$ $\bar{D}^*\Xi_c(I = 1)$ system we write the potential in the $\bar{D}^*\Xi_c$-$\bar{D}_s\Sigma_c^*$-$\bar{D}\Xi_c^*$ basis:

$$V_C(P^{\Sigma}_{cs}, J = \frac{3}{2}) = \begin{pmatrix} \tilde{d}_a & \sqrt{2}\,e_b & -e_b \\ \sqrt{2}\,e_b & \frac{2}{3}\,c_a & -\frac{\sqrt{2}}{3}\,c_a \\ -e_b & -\frac{\sqrt{2}}{3}\,c_a & \frac{1}{3}\,c_a \end{pmatrix}. \quad (73)$$

c) For the $S = -2$, $J = \frac{1}{2}$ $\bar{D}_s^*\Xi_c$ system, the basis is $\bar{D}_s\Xi_c'$-$\bar{D}\Omega_c$-$\bar{D}_s^*\Xi_c$ and the potential:

$$V_C(P^{\Xi}_{css}, J = \frac{1}{2}) = \begin{pmatrix} \frac{1}{3}\,c_a & -\frac{\sqrt{2}}{3}\,c_a & e_b \\ -\frac{\sqrt{2}}{3}\,c_a & \frac{2}{3}\,c_a & -\sqrt{2}\,e_b \\ e_b & -\sqrt{2}\,e_b & \tilde{d}_a \end{pmatrix}. \quad (74)$$

d) Finally, for $S = -2$, $J = \frac{3}{2}$ $\bar{D}_s^*\Xi_c$, we have $\bar{D}_s^*\Xi_c$-$\bar{D}_s\Xi_c^*$-$\bar{D}\Omega_c^*$ and

$$V_C(P^{\Xi}_{css}, J = \frac{3}{2}) = \begin{pmatrix} \tilde{d}_a & e_b & -\sqrt{2}\,e_b \\ e_b & \frac{1}{3}\,c_a & -\frac{\sqrt{2}}{3}\,c_a \\ -\sqrt{2}\,e_b & -\frac{\sqrt{2}}{3}\,c_a & \frac{2}{3}\,c_a \end{pmatrix}. \quad (75)$$

Here a comment is in order regarding the coupled channels containing sextet charmed baryons and charmed antimesons, which for $I = 1$, $S = -1$ and $I = \frac{1}{2}$, $S = -2$ happen to be an

admixture between octet and decuplet [69], where

$$|\bar{D}_s^{(*)}\Sigma_c^{(*)}\rangle = \sqrt{\frac{2}{3}}|8\rangle + \sqrt{\frac{1}{3}}|10\rangle\,, \tag{76}$$

$$|\bar{D}^{(*)}\Xi_c^{(\prime/*)}(1)\rangle = -\sqrt{\frac{1}{3}}|8\rangle + \sqrt{\frac{2}{3}}|10\rangle\,, \tag{77}$$

$$|\bar{D}_s^{(*)}\Xi_c^{(\prime/*)}\rangle = \sqrt{\frac{1}{3}}|8\rangle + \sqrt{\frac{2}{3}}|10\rangle\,, \tag{78}$$

$$|\bar{D}^{(*)}\Omega_c^{(*)}\rangle = -\sqrt{\frac{2}{3}}|8\rangle + \sqrt{\frac{1}{3}}|10\rangle\,, \tag{79}$$

with $|8\rangle$ and $|10\rangle$ indicating a pure octet or decuplet state, respectively. This implies that in principle the potentials in Eqs. (72-75), besides the octet coupling $c_a \equiv c_a^{(O)}$, should also contain a decuplet coupling ($c_a^{(D)}$). Yet, we have taken $c_a^{(D)} = 0$.

There are two reasons for this choice. First, for the moment there is no known hidden-charm molecular pentaquark that is a decuplet, which suggests that there might be less attraction in this configuration. This also seems to be supported by phenomenological models [16], which usually predict less attraction in the decuplets (owing to vector meson exchange being repulsive in the decuplet case). If this happens to be the case the addition of a decuplet coupling $c_a^{(D)}$ might be inconsequential after all, as the coupled channel dynamics will drive the two $\bar{H}_c S_c$ coupled channels to the octet, which is the minimum energy configuration.

Second, the decuplet configuration can be effectively ignored simply because the $\bar{H}_c T_c$ systems can only couple to the octet $\bar{H}_c S_c$ configurations, but not to the decuplet ones, which implies that the coupled channel dynamics driven by the e_b coupling vanishes if the two $\bar{H}_c S_c$ channels are in a decuplet. This is easy to show by extending the potential for the P_{cs}^{Σ} pentaquark as to include the decuplet components, which will generate a $P_{cs}^{\Sigma^*}$ pentaquark with the quantum numbers of the Σ^* decuplet light baryon, which results in

$$V_C(P_{cs}^{\Sigma^{(*)}}, J=\frac{1}{2}) = \begin{pmatrix} \frac{2}{3}\,c_a^{(O)} + \frac{1}{3}\,c_a^{(D)} & -\frac{\sqrt{2}}{3}\,(c_a^{(O)} - c_a^{(D)}) & \sqrt{2}\,e_b \\ -\frac{\sqrt{2}}{3}\,(c_a^{(O)} - c_a^{(D)}) & \frac{1}{3}\,c_a^{(O)} + \frac{2}{3}\,c_a^{(D)} & -e_b \\ \sqrt{2}\,e_b & -e_b & \tilde{d}_a \end{pmatrix}, \tag{80}$$

where now we explicitly indicate whether we are dealing with the octet or decuplet version of the c_a coupling. Here we can perform a change of basis in which the $\bar{D}_s\Sigma_c$ and $\bar{D}\Xi_c'(1)$ channels are rewritten in the octet and decuplet basis, which can be found by inverting Eqs. (76) and Eq. (77). In this new $|8(1)\rangle$-$|10(1)\rangle$-$|\bar{D}^*\Xi_c(1)\rangle$ basis (where "(1)" refers to isospin), the potential reads

$$\tilde{V}_C(P_{cs}^{\Sigma^{(*)}}, J=\frac{1}{2}) = \begin{pmatrix} c_a^{(O)} & 0 & -\sqrt{3}\,e_b \\ 0 & c_a^{(D)} & 0 \\ -\sqrt{3}\,e_b & 0 & \tilde{d}_a \end{pmatrix}, \tag{81}$$

where it is now evident that the decuplet components do not mix with the $\bar{D}\Xi_c'(1)$ ($\bar{H}_c T_c$) channel. This process can be repeated for the $J = \frac{3}{2}$ $P_{cs}^{\Sigma^{(*)}}$ configuration, as well as for $J = \frac{1}{2}$, $\frac{3}{2}$ $P_{cs}^{\Xi^{(*)}}$ ones, with identical outcomes. Of course, owing to the fact that the thresholds do not have the same mass, there will be a certain amount of mixing of octet and decuplet. Yet, we expect this to be a small effect.

From the previous two reasons — namely, that there seems to be no decuplet pentaquark and that the decuplet pentaquark configurations decouple with the configurations containing an antitriplet charmed baryon — the simplifying assumption that $c_a^{(D)} = 0$ seems a sensible choice.

After including the coupled channel dynamics suggested by the power counting estimations of Table 1 (i.e. using the potentials of Eqs. (71-75)), we obtain the predictions of Table 2. With the couplings in set A, all the $\bar{H}_c T_c$ pentaquarks will bind. The errors shown in Table 1 correspond to varying the cutoff in the $\Lambda = (0.5 - 1.0)\,\mathrm{GeV}$ window and are small, which simply indicates that the EFT is properly renormalized. These errors do not reflect the real uncertainty in the location of $\bar{H}_c T_c$ pentaquarks, as we have not explicitly considered the propagation of the experimental, HQSS ($\Lambda_{\rm QCD}/m_Q$) and EFT (Q/M) errors. Instead of including these error sources directly, we will take them into account indirectly by recalculating the $\bar{H}_c T_c$ pentaquark spectrum in two other EFTs using different inputs and counting rules. We will do this in the following section, where we will see that the actual uncertainty is of the order of tens of MeV for most of the states (as shown in Tables 3, 4 and 5).

6 Alternative power counting schemes

Power counting depends on the assumptions made about the size of different physical effects, assumptions which are in turn constrained by the experimental data available. For molecular pentaquarks there is no direct experimental data, that is, charmed antimeson - charmed baryon scattering data. This implies that there is significant freedom on how to organize their EFT description, for which the very first assumption we are relying on is that a few of the observed pentaquarks are indeed molecular. Owing to this situation, it will do no harm to revisit our initial assumptions (e.g. regarding coupled channel dynamics), propose new power counting schemes and recalculate the spectrum of the molecular pentaquarks containing an antitriplet charmed baryon. Besides power counting A, which we have described in Sect. (4), here we will propose two additional countings, B and C.

The power counting estimations of coupled channel effects we have provided up to this point have relied solely on the relative size of the propagators in a diagonal and non-diagonal channel. However, this argument ignores the relative size of the couplings connecting the channels and this distinction might be important in a few cases, as we will see. From a brief inspection of the set A determination of the c_a, d_a, $\tilde{d}_a$ and e_b couplings in Eqs. (49-52) it is apparent that the size of e_b is smaller than the other couplings. This observation might be incorporated into the power counting.

Actually, there is a phenomenological explanation for this: the contact-range couplings follow a multipolar expansion comprised of central, spin-spin and other terms associated with higher multipolar light-spin operators, which we can write schemat-

Molecule	I	S	J	Expansion parameter	Nearby thresholds		
$\bar{D}\Lambda_c$	$\frac{1}{2}$	0	$\frac{1}{2}$	0.18 (0.29)	$\bar{D}^*\Sigma_c$	$\bar{D}^*\Sigma_c^*$	–
					0.03 (0.08)	0.02 (0.07)	–
$\bar{D}^*\Lambda_c$	$\frac{1}{2}$	0	$\frac{1}{2}$	0.18 (0.42)	$\bar{D}\Sigma_c$	$\bar{D}^*\Sigma_c^*$	–
					0.35 (1.88)	0.04 (0.21)	–
$\bar{D}^*\Lambda_c$	$\frac{1}{2}$	0	$\frac{3}{2}$	0.18 (0.37)	$\bar{D}\Sigma_c^*$	$\bar{D}^*\Sigma_c^*$	–
					0.10 (0.42)	0.03 (0.16)	–
$\bar{D}_s\Lambda_c$	0	−1	$\frac{1}{2}$	0.18 (0.26)	$\bar{D}\Xi_c$	$\bar{D}^*\Xi_c'$	$\bar{D}^*\Xi_c^*$
					0.11 (0.23)	0.03 (0.06)	0.02 (0.05)
$\bar{D}_s^*\Lambda_c$	0	−1	$\frac{1}{2}$	0.18 (0.28)	$\bar{D}\Xi_c'$	$\bar{D}^*\Xi_c$	$\bar{D}^*\Xi_c'$
					0.18 (0.43)	0.11 (0.26)	0.05 (0.11)
$\bar{D}_s^*\Lambda_c$	0	−1	$\frac{3}{2}$	0.18 (0.28)	$\bar{D}^*\Xi_c$	$\bar{D}^*\Xi_c'$	$\bar{D}\Xi_c^*$
					0.11 (0.26)	0.05 (0.11)	0.08 (0.18)
$\bar{D}\Xi_c$	0	−1	$\frac{1}{2}$	0.18 (0.21)	$\bar{D}_s\Lambda_c$	$\bar{D}_s^*\Lambda_c$	-
					0.11 (0.15)	0.14 (0.20)	-
$\bar{D}^*\Xi_c$	0	−1	$\frac{1}{2}$	0.18 (0.19)	$\bar{D}\Xi_c'$	$\bar{D}_s^*\Lambda_c$	$\bar{D}_s\Lambda_c$
					0.27 (0.32)	0.11 (0.13)	0.04 (0.05)
$\bar{D}^*\Xi_c$	0	−1	$\frac{3}{2}$	0.18 (0.24)	$\bar{D}\Xi_c^*$	$\bar{D}_s^*\Lambda_c$	-
					0.24 (0.66)	0.11 (0.29)	-
$\bar{D}\Xi_c$	1	−1	$\frac{1}{2}$	0.18 (0.31)	$\bar{D}_s^*\Sigma_c$	$\bar{D}^*\Xi_c'$	$\bar{D}_s^*\Sigma_c^*$
					0.04 (0.11)	0.04 (0.10)	0.03 (0.09)
$\bar{D}^*\Xi_c$	1	−1	$\frac{1}{2}$	0.18 (0.33)	$\bar{D}_s\Sigma_c$	$\bar{D}\Xi_c'$	$\bar{D}_s^*\Sigma_c$
					0.15 (0.51)	0.27 (0.89)	0.10 (0.33)
$\bar{D}^*\Xi_c$	1	−1	$\frac{3}{2}$	0.18 (0.33)	$\bar{D}_s\Sigma_c^*$	$\bar{D}\Xi_c^*$	$\bar{D}_s^*\Sigma_c$
					1.01 (3.36)	0.24 (0.81)	0.10 (0.33)
$\bar{D}_s\Xi_c$	$\frac{1}{2}$	−2	$\frac{1}{2}$	0.18 (0.32)	$\bar{D}_s^*\Xi_c'$	$\bar{D}^*\Omega_c$	$\bar{D}_s^*\Xi_c^*$
					0.03 (0.11)	0.03 (0.10)	0.03 (0.09)
$\bar{D}_s^*\Xi_c$	$\frac{1}{2}$	−2	$\frac{1}{2}$	0.18 (0.34)	$\bar{D}_s\Xi_c'$	$\bar{D}\Omega_c$	$\bar{D}^*\Omega_c$
					0.24 (0.87)	0.44 (1.57)	0.07 (0.25)
$\bar{D}_s^*\Xi_c$	$\frac{1}{2}$	−2	$\frac{3}{2}$	0.18 (0.34)	$\bar{D}_s\Xi_c^*$	$\bar{D}\Omega_c^*$	$\bar{D}_s^*\Xi_c'$
					0.26 (0.92)	0.16 (0.58)	0.08 (0.28)

Table 1. Expansion parameter for the EFT description of the $\bar{H}_cT_c$ pentaquarks and its comparison with the expected size of the coupled channel effects of the (two or three) closest thresholds with which a given molecular pentaquark can mix. "Molecule" refers to the two-body system under consideration, I, S, J are its isospin, strangeness and spin, and the expansion parameter and relative coupled channel size are calculated as in Eqs. (26) and (27): the first number corresponds to using $Q = m_\pi$ for the calculation, while the number in parentheses uses $Q = \gamma_2$, where the wave number have been extracted either from the experimental masses (in the case of the $\bar{D}^*\Xi_c$ system), the coupled channel calculation of Eqs. (57-59) or the single channel ones of Eqs. (64-70), both of which depend on the couplings in set A, i.e. Eqs. (49-52). This determination leads to very attractive couplings, which results in a poorer expansion parameter. In contrast, other determinations will yield results closer to the $Q = m_\pi$ estimations. For the masses of the charmed baryons and mesons we use the isospin average of the values listed in the Review of Particle Physics [51].

ically as [66]

$$\langle p'|V_c|p\rangle = f_a + f_b\,\vec{S}_{L1}\cdot\vec{S}_{L2} + f_c\,Q_{L1ij}Q_{L2ij} + \dots\,, \tag{82}$$

with f_a, f_b, f_c coupling constants and where $\vec{S}_{L1(2)}$ are the light-spin operators in the vertex 1(2) and $Q_{L1(2)ij}$ are quadrupolar operators that are defined as $\frac{1}{2}(S_{L1(2)i}S_{L1(2)j} + S_{L1(2)j}S_{L1(2)i}) - \frac{1}{3}\,\delta_{ij}\vec{S}_{L1(2)}\cdot\vec{S}_{L1(2)}$, while the dots indicate higher order terms.

For the two-hadron systems we have considered, only the first two terms are non-zero (the quadrupolar term requires the light-spin of both hadrons to be $S_L \geq 1$ for it to be non-trivial). It also happens that from phenomenological arguments we expect the terms in this expansion to decrease in size as we progress in the multipolar expansion [38, 66]. That is, the size of the f_a couplings is in general larger than that of the f_b couplings, as can be appreciated for instance in Eqs. (49-52), i.e. set A. This also explains why molecular pentaquark descriptions that take $f_b = 0$ [14, 40, 70] tend to work relatively well.

The previous observation extends to coupled channels: transitions involving a coupling of the f_a type (or a-type) will be enhanced with respect to those that depend on a coupling of the f_b type (or b-type). For instance, while the $\bar{D}^*\Lambda_c$-$\bar{D}\Sigma_c$ transition depends on the coupling e_b (check Eq. (38)), this is not true for the $\bar{D}_s\Lambda_c$-$\bar{D}\Xi_c$ transition, which is proportional to the difference of the d_a and $\tilde{d}_a$ couplings. In particular, the $\bar{D}_s\Lambda_c$-$\bar{D}\Xi_c$ coupled channel potential is

$$V_C'(P_{cs}^\Lambda, I=0, S=-1) = \begin{pmatrix} \frac{1}{2}(d_a+\tilde{d}_a) & \frac{1}{\sqrt{2}}(d_a-\tilde{d}_a) \\ \frac{1}{\sqrt{2}}(d_a-\tilde{d}_a) & d_a \end{pmatrix}, \tag{83}$$

and depending on the specific values of d_a and $\tilde{d}_a$ (and how their difference compares to e_b) it could very well happen that

Molecule	I	S	J	Channel(s)	Potential	M	$M_{\rm exp}$
$\bar{D}\Lambda_c$	$\frac{1}{2}$	0	$\frac{1}{2}$	$\bar{D}\Lambda_c$	$\tilde{d}_a$	$4129.3^{+1.9}_{-0.3}$	-
$\bar{D}^*\Lambda_c$	$\frac{1}{2}$	0	$\frac{1}{2}$	$\bar{D}^*\Lambda_c$-$\bar{D}\Sigma_c$	Eq. (38)	$4246.6^{+3.6}_{-1.9}$	-
$\bar{D}^*\Lambda_c$	$\frac{1}{2}$	0	$\frac{3}{2}$	$\bar{D}^*\Lambda_c$ -$\bar{D}\Sigma_c^*$	Eq. (38)	$4257.1^{+4.0}_{-2.1}$	-
$\bar{D}\Sigma_c$	$\frac{1}{2}$	0	$\frac{1}{2}$	$\bar{D}^*\Lambda_c$-$\bar{D}\Sigma_c$	Eq. (38)	Input(M&Γ)	$4311.9-\frac{i}{2}9.8$
$\bar{D}\Sigma_c^*$	$\frac{1}{2}$	0	$\frac{3}{2}$	$\bar{D}^*\Lambda_c$ -$\bar{D}\Sigma_c^*$	Eq. (38)	$4371.4^{+0.1}_{-0.5}-\frac{i}{2}10.2^{+0.8}_{-1.8}$	$4337-\frac{i}{2}29$
$\bar{D}_s\Lambda_c$	0	-1	$\frac{1}{2}$	$\bar{D}_s\Lambda_c$	$\frac{1}{2}\left(\tilde{d}_a+d_a\right)$	$4236.1^{+0.5}_{-0.0}$	-
$\bar{D}_s^*\Lambda_c$	0	-1	$\frac{1}{2}$	$\bar{D}_s^*\Lambda_c$-$\bar{D}\Xi_c'$	Eq. (71)	$4365.6^{+2.0}_{-1.9}$	-
$\bar{D}_s^*\Lambda_c$	0	-1	$\frac{3}{2}$	$\bar{D}_s^*\Lambda_c$	$\frac{1}{2}\left(\tilde{d}_a+d_a\right)$	$4378.1^{+1.2}_{-0.5}$	-
$\bar{D}\Xi_c$	0	-1	$\frac{1}{2}$	$\bar{D}\Xi_c$	d_a	$4324.2^{+0.9}_{-1.0}$	-
$\bar{D}^*\Xi_c$	0	-1	$\frac{1}{2}$	$\bar{D}\Xi_c'$-$\bar{D}^*\Xi_c$	Eq. (40)	Input(M)$-\frac{i}{2}4.2^{+0.2}_{-0.6}$	$4467.8-\frac{i}{2}5.3$
$\bar{D}^*\Xi_c$	0	-1	$\frac{3}{2}$	$\bar{D}^*\Xi_c$-$\bar{D}\Xi_c^*$	Eq. (42)	Input(M)	$4454.9-\frac{i}{2}7.5$
$\bar{D}\Xi_c$	1	-1	$\frac{1}{2}$	$\bar{D}\Xi_c$	$\tilde{d}_a$	$4310.4^{+2.6}_{-1.0}$	-
$\bar{D}^*\Xi_c$	1	-1	$\frac{1}{2}$	$\bar{D}_s\Sigma_c$-$\bar{D}\Xi_c'$-$\bar{D}^*\Xi_c$	Eq. (72)	$4465.4^{+2.3}_{-1.4}-\frac{i}{2}17.0^{+1.1}_{-2.7}$	-
$\bar{D}^*\Xi_c$	1	-1	$\frac{3}{2}$	$\bar{D}^*\Xi_c$-$\bar{D}_s\Sigma_c^*$-$\bar{D}\Xi_c^*$	Eq. (73)	$4423.8^{+3.3}_{-3.0}$	-
$\bar{D}_s\Xi_c$	$\frac{1}{2}$	-2	$\frac{1}{2}$	$\bar{D}_s\Xi_c$	$\tilde{d}_a$	$4409.9^{+3.3}_{-1.7}$	-
$\bar{D}_s^*\Xi_c$	$\frac{1}{2}$	-2	$\frac{1}{2}$	$\bar{D}_s\Xi_c'$-$\bar{D}\Omega_c$-$\bar{D}_s^*\Xi_c$	Eq. (74)	$4572.9^{+2.0}_{-1.6}-\frac{i}{2}19.6^{+0.1}_{-1.6}$	-
$\bar{D}_s^*\Xi_c$	$\frac{1}{2}$	-2	$\frac{3}{2}$	$\bar{D}_s^*\Xi_c$-$\bar{D}_s\Xi_c^*$-$\bar{D}\Omega_c^*$	Eq. (75)	$4544.2^{+2.8}_{-1.3}$	-

Table 2. Predictions for the $\bar{H}_cT_c$ family of pentaquarks (i.e. pentaquarks containing an antitriplet baryon) and the $\bar{D}\Sigma_c^*$ system from the couplings in Eqs. (49-52), which are in turn determined from reproducing the mass and width of the $P_c(4312)$ and the masses of the two P_{cs} peaks, that is, set A of couplings (for counting A). "Channel(s)" refer to the coupled channel effects included in the calculation (which have been chosen according to their expected size as estimated in Table 1), "Potential" shows the potential in the coupled channel space, M is the calculated mass in MeV and $M_{\rm exp}$ the mass of the experimental candidates, if any (also in MeV). The central values are the prediction for $\Lambda = 0.75\,$GeV, while the errors correspond to varying the cutoff within the $(0.5-1.0)\,$GeV range.

the strength of the $\bar{D}_s\Lambda_c$-$\bar{D}\Xi_c$ dynamics is considerably larger than the naive power counting estimations. Actually, this is not the case for the couplings of Eqs. (49-52), for which the non-diagonal term in the previous potential happens to be smaller in size than e_b (but only if we accept the attractive $\tilde{d}_a$ solution to the fit we made). Yet, this might be fortuitous, as Eqs. (49-52) display relative similar values for d_a and $\tilde{d}_a$.

Owing to the fact that the $(d_a-\tilde{d}_a)/\sqrt{2}$ combination of couplings might be larger than expected, it is a good idea to consider this type of coupled channel dynamics explicitly. Besides, its dependence on the relative signs of the d_a and $\tilde{d}_a$ couplings makes this coupled channel particularly relevant to explore whether the $\bar{D}^{(*)}\Lambda_c$ diagonal interaction is attractive or repulsive. First, we will do this in a scheme in which we set $e_b = 0$, as we expect this b-type coupling to be smaller in size to the a-type couplings. This will be power counting B. From this we will reproduce the mass and width of the single peak solution of the $P_{cs}(4459)$ pentaquark, i.e. Eq. (12), leading to set B:

$$d_a = 1.35\,(1.67-1.23)\,c_a^{\rm ref}\,, \tag{84}$$

$$\tilde{d}_a = 0.67\,(0.52-0.74)\,c_a^{\rm ref}\,. \tag{85}$$

These values in turn lead to the predictions of Table 3 .

Second, we will consider the case in which all the assumptions behind power counting B hold, except that now we will take $e_b \neq 0$ again. We will call this choice power counting C. In this case the $J=\frac{1}{2}$ and $\frac{3}{2}$ P_{cs} pentaquarks are $\bar{D}_s^*\Lambda_c$-$\bar{D}\Xi_c'$-$\bar{D}^*\Xi_c$ and $\bar{D}_s^*\Lambda_c$-$\bar{D}^*\Xi_c$-$\bar{D}\Xi_c^*$ molecules, respectively, with potentials

$$V_C(P_{cs}, J=\frac{1}{2}) = \begin{pmatrix} \frac{1}{2}(d_a+\tilde{d}_a) & -\sqrt{2}\,e_b & \frac{1}{\sqrt{2}}(d_a-\tilde{d}_a) \\ -\sqrt{2}\,e_b & c_a & e_b \\ \frac{1}{\sqrt{2}}(d_a-\tilde{d}_a) & e_b & d_a \end{pmatrix}, \tag{86}$$

$$V_C(P_{cs}, J=\frac{3}{2}) = \begin{pmatrix} \frac{1}{2}(d_a+\tilde{d}_a) & \frac{1}{\sqrt{2}}(d_a-\tilde{d}_a) & -\sqrt{2}\,e_b \\ \frac{1}{\sqrt{2}}(d_a-\tilde{d}_a) & d_a & e_b \\ -\sqrt{2}\,e_b & e_b & c_a \end{pmatrix}. \tag{87}$$

Now we have four parameters that can be determined from different inputs, including the $P_c(4312)$ and the P_{cs1} and P_{cs2}. Here, for a better comparison with the previous calibration (with $e_b = 0$) we will use the two-peak $P_{cs}(4459)$ solution and determine the four couplings to the masses and widths of the P_c and P_{cs1} (set C_1):

$$c_a = 1.09\,(1.14-1.06)\,c_a^{\rm ref}\,, \tag{88}$$

$$d_a = 1.28\,(1.49-1.19)\,c_a^{\rm ref}\,, \tag{89}$$

$$\tilde{d}_a = 0.76\,(0.66-0.81)\,c_a^{\rm ref}\,, \tag{90}$$

$$e_b = \pm 0.14\,(0.20-0.11)\,c_a^{\rm ref}\,, \tag{91}$$

or alternatively with P_c and P_{cs2} (set C_2):

$$c_a = 1.10\,(1.16 - 1.07)\,c_a^{\rm ref}\,, \quad (92)$$
$$d_a = 1.04\,(1.10 - 1.02)\,c_a^{\rm ref}\,, \quad (93)$$
$$\tilde{d}_a = 0.79\,(0.71 - 0.83)\,c_a^{\rm ref}\,, \quad (94)$$
$$e_b = \pm 0.15\,(0.21 - 0.12)\,c_a^{\rm ref}\,, \quad (95)$$

or directly from P_{cs1} and P_{cs2} (set C_3):

$$c_a = 1.33\,(1.54 - 1.23)\,c_a^{\rm ref}\,, \quad (96)$$
$$d_a = 1.10\,(1.22 - 1.06)\,c_a^{\rm ref}\,, \quad (97)$$
$$\tilde{d}_a = 1.28\,(1.63 - 1.17)\,c_a^{\rm ref}\,, \quad (98)$$
$$e_b = \pm 0.35\,(0.56 - 0.25)\,c_a^{\rm ref}\,, \quad (99)$$

where the couplings are largely compatible with those of set B in Eqs. (84) and (85). In every case, we have chosen the solution with a smaller value of $|e_b|$ if there is more than one solution (as to represent a perturbation over counting B and set B). We see that sets C_1 and C_3 are similar to sets B and A, respectively, while set C_2 is the one closest to the phenomenological expectations that we discussed in Eqs. (53-56), in particular that $c_a \sim d_a$ and $|c_a|, |d_a| > |\tilde{d}_a|$, which might suggest that set C_2 is the most satisfactory of the three fits. Thus we will choose set C_2 for calculating the spectrum, which we show in Table 4. The predictions happen to be qualitatively similar to those of set A and B, Tables 2 and 3, but leading to heavier molecular pentaquarks (i.e. to less binding energy) and to a smaller hyperfine splitting between the P_{cs1} and P_{cs2} pentaquarks than set A.

Finally, we compare the $\Lambda = 0.75\,\text{GeV}$ (central value) predictions of all the five determinations of the couplings in Table 5. A few remarks are in order: first, (i) the qualitative characteristics of the spectrum are similar for all five determinations of the couplings. Second, (ii) the largest quantitative differences happen for the molecular configurations that depend on the $\tilde{d}_a$ coupling, which is only determined indirectly by its effect on the width of $P_c(4312)$ or P_{cs1} and P_{cs2}. Then, (iii) all this depends on the assumptions we are making in the first place to determine the couplings, i.e. that the pentaquarks used as input are all indeed meson-baryon bound states. It might very well happen that this is not the case, or that the masses, widths or quantum numbers of the pentaquarks we are using as input might also change in future experiments. The bottom-line is that the predictions of $\bar{H}_c T_c$ pentaquarks we present here are tentative in nature.

7 Conclusions

From a theoretical point of view, the new $P_c(4337)$ pentaquark is more puzzling than the previous $P_c(4312)$, $P_c(4440)$, $P_c(4457)$ and $P_{cs}(4459)$ pentaquarks. While the later are easily explained as $\bar{D}\Sigma_c$, $\bar{D}^*\Sigma_c$ and $\bar{D}^*\Xi_c$ bound states (which does not necessarily mean they are), the new $P_c(4337)$ does not fit into the previous pattern so nicely. From HQSS we expect the existence of a $\bar{D}\Sigma_c^*$ bound state, yet its mass is usually predicted to lie in the $4370 - 4380\,\text{MeV}$ range, about $30 - 40\,\text{MeV}$ above the mass of the $P_c(4337)$. Thus the $P_c(4337)$ offers a more interesting challenge than the other pentaquarks.

Here we explore a few explanations of the new $P_c(4337)$: (i) that it is a $\chi_{c0}p$ bound state, (ii) that, owing to the Breit-Wigner parametrization being not suitable to near threshold states, the $P_c(4337)$ is actually a $\bar{D}\Sigma_c$ molecule while the $P_c(4312)$ is a $\bar{D}^*\Lambda_c$ molecule instead and (iii) that the $P_c(4312)$ and $P_c(4337)$ are actually a consequence of the $\bar{D}^*\Lambda_c$-$\bar{D}\Sigma_c$ and $\bar{D}^*\Lambda_c$-$\bar{D}\Sigma_c^*$ coupled channel dynamics.

The first explanation, which requires $J^P = \frac{1}{2}^+$ for the $P_c(4337)$, is theoretically plausible and has the advantage of leaving the usual molecular understanding of the $P_c(4312)$, $P_c(4440)$, $P_c(4457)$ and $P_{cs}(4459)$ pentaquarks unchanged, as the new $P_c(4337)$ will be unrelated to the previous pentaquarks. If this is the case, in analogy to the results of Ref. [7] for $\psi' p$, other $\chi_{c0}B_8$, $\chi_{c1}B_8$ and $\chi_{c2}B_8$ pentaquarks are to be expected, with B_8 representing baryons in the light baryon octet. This explanation has been recently explored in Ref. [5], for instance (though in this reference the $P_c(4337)$ happens to be related to the $P_{cs}(4459)$, which is not the case in the present work).

The second explanation is grounded in the observation that the difference in the masses of the $P_c(4312)$ and $P_c(4337)$ states coincides with the mass gap of the $\bar{D}^*\Lambda_c$ and $\bar{D}\Sigma_c$ thresholds. It implies $J^P = \frac{1}{2}^-$ for the $P_c(4337)$, while suggesting a $J^P = \frac{1}{2}^-$ and $\frac{3}{2}^-$ double peak nature of the $P_c(4312)$ (i.e. the two spin states of $\bar{D}^*\Lambda_c$), which is an interesting possibility. Besides, it will imply a strong attractive interaction for all the $\bar{H}_c T_c = \bar{D}^{(*)}\Lambda_c$, $\bar{D}_s^{(*)}\Lambda_c$, $\bar{D}^{(*)}\Xi_c$ and $\bar{D}_s^{(*)}\Xi_c$ systems and thus the existence of a few new molecular pentaquarks. For checking this possibility it will be necessary to adapt the techniques of Refs. [29–31] to the particular case of the previous two channels and pentaquarks.

The third explanation hopes to reproduce the $P_c(4312)$ and $P_c(4337)$ pentaquarks as poles in the $\bar{D}^*\Lambda_c$-$\bar{D}\Sigma_c$ and $\bar{D}^*\Lambda_c$-$\bar{D}\Sigma_c^*$ coupled channel systems. This requires the $P_c(4312)$ and $P_c(4337)$ to have $J^P = \frac{1}{2}^-$ and $\frac{3}{2}^-$, respectively. Though this explanation fails to reproduce the location of the $P_c(4337)$ accurately, it nonetheless shows that the $P_c(4312)$ and the double peak interpretation of the $P_{cs}(4459)$ can be described with the same set of parameters in the molecular picture. Actually, the aforementioned failure might be attributable to a very prosaic explanation: the non-relativistic EFT we are using to describe the $P_c(4312)$ and $P_c(4337)$ states might converge better in the former than in the later. In fact, the LO uncertainty in the mass of the $P_c(4337)$ as a $\bar{D}\Sigma_c^*$ molecule could be compatible with its experimental location, at least for pessimistic estimations of these uncertainties. This is not what we could call a very exciting conclusion, but it is not a particularly plausible interpretation either once we consider more sober estimations of the LO errors. Indeed, for most calculations the preferred mass of the $\bar{D}\Sigma_c^*$ molecule is consistently centered around $(4370{-}4380)\,\text{MeV}$, in agreement with previous theoretical works [13, 16–19] (and in disagreement with the hypothesis of the $P_c(4337)$ being a $\bar{D}\Sigma_c^*$ molecule). Nonetheless it is still true that the $\bar{D}^*\Lambda_c$-$\bar{D}\Sigma_c^*$ explanation points again towards the existence of a few unobserved molecular pentaquarks involving the antitriplet charmed baryons. Using different power countings for the coupled channel effects and inputs, we have calculated a series of possible predictions for the masses of these pentaquarks.

Molecule	I	S	J	Channel(s)	Potential	M	$M_{\rm exp}$
$\bar{D}\Lambda_c$	$\frac{1}{2}$	0	$\frac{1}{2}$	$\bar{D}\Lambda_c$	$\tilde{d}_a$	$(4153.7^{+0.0}_{-0.0})^V$	-
$\bar{D}^*\Lambda_c$	$\frac{1}{2}$	0	$\frac{1}{2},\frac{3}{2}$	$\bar{D}^*\Lambda_c$	$\tilde{d}_a$	$4295.0^{+0.1}_{-0.0}$	-
$\bar{D}_s\Lambda_c$	0	-1	$\frac{1}{2}$	$\bar{D}_s\Lambda_c$-$\bar{D}\Xi_c$	Eq. (83)	$4233.6^{+2.6}_{-6.7}$	-
$\bar{D}_s^*\Lambda_c$	0	-1	$\frac{1}{2},\frac{3}{2}$	$\bar{D}_s^*\Lambda_c$-$\bar{D}^*\Xi_c$	Eq. (83)	$4374.9^{+1.8}_{-6.1}$	
$\bar{D}\Xi_c$	0	-1	$\frac{1}{2}$	$\bar{D}_s\Lambda_c$-$\bar{D}\Xi_c$	Eq. (83)	$4319.0^{+0.7}_{-0.8} - \frac{i}{2}(16.9 \pm 0.2)$	-
$\bar{D}^*\Xi_c$	0	-1	$\frac{1}{2},\frac{3}{2}$	$\bar{D}_s^*\Lambda_c$-$\bar{D}^*\Xi_c$	Eq. (83)	Input(M&Γ)	$4458.8 - \frac{i}{2}17.3$
$\bar{D}\Xi_c$	1	-1	$\frac{1}{2}$	$\bar{D}\Xi_c$	$\tilde{d}_a$	$4336.6^{+0.1}_{-0.0}$	-
$\bar{D}^*\Xi_c$	1	-1	$\frac{1}{2},\frac{3}{2}$	$\bar{D}^*\Xi_c$	$\tilde{d}_a$	$4477.8^{+0.2}_{-0.1}$	-
$\bar{D}_s\Xi_c$	$\frac{1}{2}$	-2	$\frac{1}{2}$	$\bar{D}_s\Xi_c$	$\tilde{d}_a$	$4437.6^{+0.2}_{-0.1}$	-
$\bar{D}_s^*\Xi_c$	$\frac{1}{2}$	-2	$\frac{1}{2},\frac{3}{2}$	$\bar{D}_s^*\Xi_c$	$\tilde{d}_a$	$4581.2^{+0.4}_{-0.3}$	-

Table 3. Predictions of the $\bar{H}_cT_c$ pentaquarks from the fit to the $P_{cs}(4459)$ mass and width in the single peak solution, i.e. set B in Eqs. (84) and (85) for counting B. We refer to Table 2 for the conventions we have used ("Molecule", I, S, J, etc. as well as the cutoff and the uncertainties). The only new convention we use is the superscript ^{V}, which indicates that the pole is a virtual state (instead of a bound state).

Molecule	I	S	J	Channel(s)	Potential	M	$M_{\rm exp}$
$\bar{D}\Lambda_c$	$\frac{1}{2}$	0	$\frac{1}{2}$	$\bar{D}\Lambda_c$	$\tilde{d}_a$	$4152.4^{+0.4}_{-0.0}$	-
$\bar{D}^*\Lambda_c$	$\frac{1}{2}$	0	$\frac{1}{2}$	$\bar{D}^*\Lambda_c$-$\bar{D}\Sigma_c$	Eq. (38)	$4286.4^{+0.4}_{-0.0}$	-
$\bar{D}^*\Lambda_c$	$\frac{1}{2}$	0	$\frac{3}{2}$	$\bar{D}^*\Lambda_c$ -$\bar{D}\Sigma_c^*$	Eq. (38)	$4291.4^{+0.4}_{-0.0}$	-
$\bar{D}\Sigma_c$	$\frac{1}{2}$	0	$\frac{1}{2}$	$\bar{D}^*\Lambda_c$-$\bar{D}\Sigma_c$	Eq. (38)	Input (M & Γ)	$4311.9 - \frac{i}{2}9.8$
$\bar{D}\Sigma_c^*$	$\frac{1}{2}$	0	$\frac{3}{2}$	$\bar{D}^*\Lambda_c$ -$\bar{D}\Sigma_c^*$	Eq. (38)	$4373.6 - \frac{i}{2}5.2^{+6.2}_{-2.3}$	$4337 - \frac{i}{2}29$
$\bar{D}_s\Lambda_c$	0	-1	$\frac{1}{2}$	$\bar{D}_s\Lambda_c$	Eq. (83)	$4248.3^{+0.7}_{-0.9}$	-
$\bar{D}_s^*\Lambda_c$	0	-1	$\frac{1}{2}$	$\bar{D}_s^*\Lambda_c$-$\bar{D}\Xi_c'$-$\bar{D}^*\Xi_c$	Eq. (86)	$4388.5^{+0.2}_{-0.2}$	-
$\bar{D}_s^*\Lambda_c$	0	-1	$\frac{3}{2}$	$\bar{D}_s^*\Lambda_c$-$\bar{D}^*\Xi_c$-$\bar{D}\Xi_c^*$	Eq. (87)	$4389.9^{+0.2}_{-0.3}$	-
$\bar{D}\Xi_c$	0	-1	$\frac{1}{2}$	$\bar{D}_s\Lambda_c$-$\bar{D}\Xi_c$	Eq. (83)	$4326.8^{+0.2}_{-0.9} - \frac{i}{2}1.0^{+0.1}_{-0.0}$	-
$\bar{D}^*\Xi_c$	0	-1	$\frac{1}{2}$	$\bar{D}_s^*\Lambda_c$-$\bar{D}\Xi_c'$-$\bar{D}^*\Xi_c$	Eq. (86)	Input(M&Γ)	$4467.8 - \frac{i}{2}5.3$
$\bar{D}^*\Xi_c$	0	-1	$\frac{3}{2}$	$\bar{D}_s^*\Lambda_c$-$\bar{D}^*\Xi_c$-$\bar{D}\Xi_c^*$	Eq. (87)	$4463.9^{+0.7}_{-0.3} - \frac{i}{2}0.8^{+0.1}_{-0.0}$	$4454.9 - \frac{i}{2}7.5$
$\bar{D}\Xi_c$	1	-1	$\frac{1}{2}$	$\bar{D}\Xi_c$	$\tilde{d}_a$	$4334.8^{+0.2}_{-0.0}$	-
$\bar{D}^*\Xi_c$	1	-1	$\frac{1}{2}$	$\bar{D}_s\Sigma_c$-$\bar{D}\Xi_c'$-$\bar{D}^*\Xi_c$	Eq. (72)	$4477.2^{+0.3}_{-0.0} - \frac{i}{2}3.1^{+0.1}_{-0.4}$	-
$\bar{D}^*\Xi_c$	1	-1	$\frac{3}{2}$	$\bar{D}^*\Xi_c$-$\bar{D}_s\Sigma_c$-$\bar{D}\Xi_c^*$	Eq. (73)	$4463.8^{+0.7}_{-0.1}$	-
$\bar{D}_s\Xi_c$	$\frac{1}{2}$	-2	$\frac{1}{2}$	$\bar{D}_s\Xi_c$	$\tilde{d}_a$	$4435.4^{+0.4}_{-0.0}$	-
$\bar{D}_s^*\Xi_c$	$\frac{1}{2}$	-2	$\frac{1}{2}$	$\bar{D}_s\Xi_c'$-$\bar{D}\Omega_c$-$\bar{D}_s^*\Xi_c$	Eq. (74)	$4582.2^{+0.1}_{-0.0} - \frac{i}{2}6.1^{+0.1}_{-0.5}$	-
$\bar{D}_s^*\Xi_c$	$\frac{1}{2}$	-2	$\frac{3}{2}$	$\bar{D}_s^*\Xi_c$-$\bar{D}_s\Xi_c^*$-$\bar{D}\Omega_c^*$	Eq. (75)	$4577.3^{+0.2}_{-0.0}$	-

Table 4. Predictions of the $\bar{H}_cT_c$ pentaquarks (plus the $\bar{D}\Sigma_c$ and $\bar{D}\Sigma_c^*$ systems) from the fit to the $P_c(4312)$ and P_{cs2} masses and widths, i.e. set C_2 in Eqs. (92-95) for counting C. We refer to Table 2 for the conventions we have used ("Molecule", I, S, J, etc. as well as the cutoff and the uncertainties).

The EFT description of the $P_c(4312)$ and $P_c(4337)$ as $\bar{D}^*\Lambda_c$-$\bar{D}\Sigma_c$ and $\bar{D}^*\Lambda_c$-$\bar{D}\Sigma_c^*$ systems depends on how we count coupled channel effects. Within EFT, the inclusion of coupled channel dynamics depends on two factors, the mass difference between the two channels and the relative size of the transition potential. The first factor is straightforward: a larger mass difference between thresholds implies a larger suppression of a given coupled channel effect. For the second factor, the transition potential, we have considered three power countings, A, B and C: A assumes that the antitriplet-sextet charmed baryon transitions (e.g. $\bar{D}^*\Lambda_c$-$\bar{D}\Sigma_c$) are enhanced with respect to naive expectations, B in contrast chooses to enhance the antitriplet-antitriplet transitions (e.g. $\bar{D}_s^*\Lambda_c$-$\bar{D}^*\Xi_c$), while C enhances both. While the mass of the $\bar{D}\Sigma_c^*$ molecule is fairly independent of which choice we have made among the previous countings, this is not the case for all the meson-baryon systems we have considered here. For instance, owing to the closeness of the thresholds involved, the predictions for the mass of the $I = 1$, $J = \frac{3}{2}$ $\bar{D}^*\Xi_c$-$\bar{D}_s\Sigma_c^*$-$\bar{D}\Xi_c^*$ bound state vary by a few tens of MeV depending on the coupled channel dynamics and hence, on which counting we use. Finally, the impact of pion exchanges (particularly tensor OPE) remains a very interesting subject for future investigations: though we suspect that pion exchanges might be perturbative, this is yet to be proven with explicit comparisons between perturbative and non-perturbative calculations.

Acknowledgments

We thank Feng-Kun Guo for comments and suggestions. M.P.V. would also like to thank the IJCLab of Orsay, where part of this work has been done, for its long-term hospitality. This work is partly supported by the National Natural Science Foundation of China under Grants No. 11735003, No. 11835015,

Molecule	I	S	J	Set A	Set B	Set C_1	Set C_2	Set C_3
$\bar{D}\Lambda_c$	$\frac{1}{2}$	0	$\frac{1}{2}$	4129.3	$(4153.7)^V$	4153.0	4152.4	4131.4
$\bar{D}^*\Lambda_c$	$\frac{1}{2}$	0	$\frac{1}{2}$	4246.6	4295.0	4288.2	4286.4	4238.1
$\bar{D}^*\Lambda_c$	$\frac{1}{2}$	0	$\frac{3}{2}$	4257.1	4295.0	4292.5	4291.4	4252.9
$\bar{D}\Sigma_c$	$\frac{1}{2}$	0	$\frac{1}{2}$	Input(M&Γ)	-	Input(M&Γ)	Input(M&Γ)	4313.6
$\bar{D}\Sigma_c^*$	$\frac{3}{2}$	0	$\frac{1}{2}$	4371.4	-	4373.6	4373.6	4371.2
$\bar{D}_s\Lambda_c$	0	-1	$\frac{1}{2}$	4236.1	4233.6	4238.2	4248.3	4235.5
$\bar{D}_s^*\Lambda_c$	0	-1	$\frac{1}{2}$	4365.6	4374.9	4378.5	4388.5	4354.4
$\bar{D}_s^*\Lambda_c$	0	-1	$\frac{3}{2}$	4378.1	4374.9	4379.2	4389.9	4365.2
$\bar{D}\Xi_c$	0	-1	$\frac{1}{2}$	4324.2	4319.0	4318.5	4326.8	4323.4
$\bar{D}^*\Xi_c$	0	-1	$\frac{1}{2}$	Input(M)	Input(M&Γ)	4460.2	Input(M&Γ)	Input(M&Γ)
$\bar{D}^*\Xi_c$	0	-1	$\frac{3}{2}$	Input(M)	Input(M&Γ)	Input(M&Γ)	4463.9	Input(M&Γ)
$\bar{D}\Xi_c$	1	-1	$\frac{1}{2}$	4310.4	4336.6	4335.5	4334.8	4312.5
$\bar{D}^*\Xi_c$	1	-1	$\frac{1}{2}$	4465.4	4477.8	4477.6	4477.2	4471.6
$\bar{D}^*\Xi_c$	1	-1	$\frac{3}{2}$	4423.8	4477.8	4465.6	4463.8	4414.5
$\bar{D}_s\Xi_c$	$\frac{1}{2}$	-2	$\frac{1}{2}$	4409.9	4437.6	4436.2	4435.4	4412.0
$\bar{D}_s^*\Xi_c$	$\frac{1}{2}$	-2	$\frac{1}{2}$	4572.9	4581.2	4582.6	4582.2	4580.4
$\bar{D}_s^*\Xi_c$	$\frac{1}{2}$	-2	$\frac{3}{2}$	4544.2	4581.2	4578.5	4577.3	4551.4

Table 5. Comparison of the predictions of the $\bar{H}_cT_c$ pentaquarks (plus the $\bar{D}\Sigma_c$ and $\bar{D}\Sigma_c^*$ systems) from the five determinations of the couplings we have considered, i.e. set A (Eqs. (49-52)), B (Eqs. (84-85)), C_1 (Eqs. (88-91)), C_2 (Eqs. (92-95)) and C_3 (Eqs. (96-99)). We refer to Table 2 for the conventions we have used ("Molecule", I, S, J, etc.). As for the cutoff, we take $\Lambda = 0.75\,\text{GeV}$. The differences among the predictions for each set could be interpreted as the expected theoretical uncertainty for the masses of these pentaquarks.

No. 11975041, No. 12047503 and No. 12125507, the Chinese Academy of Sciences under Grant No. XDPB15, the Fundamental Research Funds for the Central Universities and the Thousand Talents Plan for Young Professionals.

A Subleading order contributions to the molecular pentaquark potential

In this appendix we briefly review the subleading order potential for the anticharmed meson and charmed baryon system. If we consider the contact-range potential first, the operators with up to two derivatives (i.e. containing up to $\vec{q}^{\,2}$ terms) that are pertinent to the molecular pentaquarks we are considering here are

$$\begin{aligned} V_C(\vec{q}, \bar{H}_c S_c) &= \hat{c}_a + \hat{c}_{a2}\,\vec{q}^{\,2} \\ &+ \left(\hat{c}_b + \hat{c}_{b2}\,\vec{q}^{\,2}\right)\vec{\sigma}_{L1}\cdot\vec{S}_{L2} \\ &+ \hat{c}_{c2}\left(\vec{\sigma}_{L1}\cdot\vec{q}\,\vec{S}_{L2}\cdot\vec{q} - \frac{1}{3}\vec{\sigma}_{L1}\cdot\vec{S}_{L2}\,\vec{q}^{\,2}\right) \\ &+ \hat{c}_{d2}\,Q_{L2ij}\,q_i\,q_j\,, \end{aligned} \tag{100}$$

$$V_C(\vec{q}, \bar{H}_c T_c) = \hat{d}_a + \hat{d}_{a2}\,\vec{q}^{\,2}\,, \tag{101}$$

$$\begin{aligned} V_C(\vec{q}, \bar{H}_c T_c - \bar{H}_c S_c) &= \left(\hat{e}_b + \hat{e}_{b2}\,\vec{q}^{\,2}\right)\vec{\sigma}_{L1}\cdot\vec{\epsilon}_{L2} \\ &+ \hat{e}_{c2}\left(\vec{\sigma}_{L1}\cdot\vec{q}\,\vec{\epsilon}_{L2}\cdot\vec{q} - \frac{1}{3}\vec{\sigma}_{L1}\cdot\vec{\epsilon}_{L2}\,\vec{q}^{\,2}\right), \end{aligned} \tag{102}$$

where by pertinent we refer to S-wave or S-to-D-wave operators (in addition to these there will be P-wave operators too, but they are unrelated to the S-wave bound states we are dealing with here). In the expressions above $\hat{c}$, $\hat{d}$ and $\hat{e}$ are short-hand for their SU(3)-flavor decomposition, which we have not written down explicitly, $\vec{q}$ is the momentum exchanged between the hadrons, $\vec{\sigma}_{L1}$ are the Pauli matrices as applied to the light-spin of the $\bar{D}$ and $\bar{D}^*$ mesons, $\vec{\epsilon}_{L2}$ and $\vec{S}_{L2}$ the polarization vector and the spin operator of the light diquark within the sextet charmed baryons and Q_{L2ij} a quadrupolar light-spin operator defined as

$$Q_{L2ij} = \frac{1}{2}(S_{L2i}S_{L2j} + S_{L2j}S_{L2i}) - \frac{1}{3}\vec{S}^2_{L2}\delta_{ij}\,. \tag{103}$$

Each of these contacts work as follows:

a) The $\hat{c}_a$, $\hat{d}_a$, $\hat{e}_b$ contacts and their derivative counterparts ($\hat{c}_{a2}$, $\hat{d}_{a2}$, $\hat{e}_{b2}$) only act on S-waves.
b) This is also the case for $\hat{c}_b$ and $\hat{c}_{b2}$, which generate the hyperfine splitting among the different spin configurations of the $\bar{D}^*\Sigma_c$ and $\bar{D}^*\Sigma_c^*$ systems. However, we do not consider these systems here.
c) The $\hat{c}_{c2}$ contact generates S-to-D-wave mixing in the $\bar{D}^*\Sigma_c$ and $\bar{D}^*\Sigma_c^*$ systems (and the transitions of the previous two systems to and from the $\bar{D}\Sigma_c$ and $\bar{D}\Sigma_c^*$). Thus $\hat{c}_{c2}$ is not of direct relevance for this work either.
d) The $\hat{c}_{d2}$ contact also provides S-to-D-wave mixing, but it affects the $\bar{D}\Sigma_c^*$ and $\bar{D}^*\Sigma_c^*$ systems instead, i.e. systems containing a Σ_c^* (and the transitions to and from $\bar{D}\Sigma_c$ and $\bar{D}^*\Sigma_c$). It will generate a bit of attraction in $\bar{D}\Sigma_c^*$, though at subleading orders only.
e) Finally, the $\hat{e}_{c2}$ contact represents an S-to-D-wave transition between $\bar{D}^*\Lambda_c$ and $\bar{D}\Sigma_c$, $\bar{D}\Sigma_c^*$, etc.

All this means that the couplings directly relevant for the molecular pentaquarks we are considering here are the octet piece of $\hat{c}_a$, $\hat{c}_{a2}$ and $\hat{c}_{d2}$, the singlet and octet pieces of $\hat{d}_a$ and $\hat{d}_{a2}$ and the octet piece of $\hat{e}_b$, $\hat{e}_{b2}$ and $\hat{e}_{c2}$, meaning a total of 10 independent couplings with less than two derivatives. The previous number

assumes that the power counting is determined by naive dimensional analysis (NDA), i.e. terms with no derivatives count as Q^0 and terms with two derivatives as Q^2.

However, if we are dealing with non-perturbative physics, the previous assumptions about the power counting do not apply, as already discussed in Sect. 4.1 for the LO couplings. Here, we will briefly explain the power counting of the subleading couplings from a Wilsonian renormalization group (RG) point of view [71–73]. That is, we will consider the evolution of the contact-range couplings as we soften the cutoff under the constraint that observable quantities remain cutoff independent. If we have a theory with soft and hard momentum scales Q and M, where $M \gg Q$, and use a momentum space cutoff Λ to regularize the loop integrals, first we will begin by assuming that when the cutoff is of the order of the hard scale, $\Lambda \sim M$, the contact-range couplings are natural in M [73, 74]

$$c_d(\Lambda \sim M) \propto \frac{1}{M^{2+d}}\,, \tag{104}$$

where d is the number of derivatives of the contact-range operator that multiplies the coupling c_d. As the cutoff evolves towards $\Lambda \sim Q$, the contributions that originally were in the loops will be reabsorbed in the couplings themselves, leading to a change in their value

$$c_d(\Lambda \sim Q) \propto \frac{1}{M^{2+d}} \left(\frac{M}{Q}\right)^a\,, \tag{105}$$

where we have assumed a power-law evolution for simplicity. If $a > 0$, this coupling will be enhanced at low energies by a factor of $1/Q^a$ in the counting; this usually happens in the presence of non-perturbative physics, which depend on loops. Hence, as loop contributions are reduced as the cutoff softens, the couplings have to compensate by increasing their contribution. Of course, it is important to notice that here the cutoff is being used as an *analysis tool*: we reduce Λ to uncover which couplings are more relevant at low energies. Its use is different than in standard calculations, for which $\Lambda > Q$ is necessary to avoid finite cutoff effects at low energies. We notice that the standard expectation of no divergences at large Λ for a renormalized calculation is fulfilled within the Wilsonian approach. By virtue of the RG evolution being derived from the cutoff independence of observables, and provided we have included all couplings required at the order we are calculating, there should be cutoff independence (modulo higher order corrections) when the cutoff is increased to $\Lambda \sim M$.

In this picture, if we reconsider the $P_c(4312)$ and $P_{cs}(4459)$ as $\bar{D}\Sigma_c$ and $\bar{D}^*\Xi_c$ shallow bound states, respectively, we end up with

$$c_a(\Lambda), d_a(\Lambda) \propto \frac{2\pi}{\mu}\,\frac{1}{\Lambda}\,, \tag{106}$$

with μ the reduced mass of any of these two systems and Λ the cutoff, where the previous expression can be derived from Eqs. (18) and (19) and taking the binding energy equal to zero for simplicity. In contrast, in Sect. 4.1 we discussed instead the renormalized couplings, for which we basically ignored the cutoff in Eqs. (18) and (19), leading to Eq. (20). Yet, the end result in terms of power counting is the same, because as we reduce the cutoff to $\Lambda \sim Q$, we find

$$c_a, d_a \sim Q^{-1}\,, \tag{107}$$

to which we also have also added

$$\tilde{d}_a, e_b \sim Q^{-1}\,, \tag{108}$$

where the promotion of $\tilde{d}_a$ implicitly assumes a bound or virtual state in the $\bar{D}\Lambda_c$ system. Meanwhile, the promotion of e_b is not strictly required but will nonetheless be useful if we want to describe the hyperfine splitting of the P_{cs1} and P_{cs2} pentaquarks at LO. This leave us with 4 couplings at LO (or Q^{-1}). Despite this picture being very different from the more standard one that we laid out in Sect. 4.1, they nonetheless arrive to the same conclusion.

For NLO (or Q^0) we have to take into account that the counting of the contacts involving two derivatives is affected by the LO wave functions. In particular they will be promoted, as we can check by imposing renormalization group invariance to these couplings. The idea is that if we have a subleading order contact-range interaction of the form

$$\delta V_C = \delta c(\Lambda) \times O_{12}(\vec{q}^2)\,, \tag{109}$$

where $\delta c(\Lambda)$ is a subleading order coupling and O_{12} a contact-range operator involving at least two derivatives, then the running of $\delta c(\Lambda)$ can be determined from the condition [72]

$$\frac{d}{d\Lambda}\,\langle \Psi'_{\rm LO}|\,\delta V_C|\Psi_{\rm LO}\rangle = 0\,, \tag{110}$$

where $|\Psi_{\rm LO}\rangle$ and $|\Psi'_{\rm LO}\rangle$ refer to the initial and final LO wave functions. That is, the matrix elements of δV_C should be cutoff independent. Usually, the evaluation of this matrix element leads to an equation of the type

$$\frac{d}{d\Lambda}\,\left[\Lambda^a\,\delta c(\Lambda)\right] = 0\,, \tag{111}$$

which implies an enhancement of $\delta c(\Lambda)$ by a factor of $1/Q^a$ as we evolve it from $\Lambda \sim M$ to $\Lambda \sim Q$. The enhancement is easy to deduce from the expected behavior of the S- and D-wave wave functions [73], yielding:

a) $1/Q^1$ ($a = 1$) for the S-to-D-wave couplings ($\hat{c}_{d2}$, $\hat{e}_{c2}$) and
b) $1/Q^2$ ($a = 2$) for the S-wave couplings ($\hat{c}_{a2}$, $\hat{d}_{a2}$, $\hat{e}_{b2}$).

As a consequence, the S-wave couplings are promoted from Q^2 to Q^0 (or NLO), while all the tensor and quadrupolar operators are promoted from Q^2 to Q^1 (or N^{2}LO). This leave us with only 4 new couplings (or a total of 8) at NLO and 2 more (or a total of 10) at N^{2}LO. The enhancement we find here for the S- and S-to-D-wave derivative interactions is identical to the one previously calculated in the two-nucleon system when OPE is either perturbative [42, 43] or not present [75], despite the obvious differences in the methodology.

References

1. R. Aaij *et al.* (LHCb), Phys. Rev. Lett. **128**, 062001 (2022), arXiv:2108.04720 [hep-ex] .

2. R. Aaij *et al.* (LHCb), Phys. Rev. Lett. **122**, 222001 (2019), arXiv:1904.03947 [hep-ex] .
3. R. Aaij *et al.* (LHCb), Sci. Bull. **66**, 1391 (2021), arXiv:2012.10380 [hep-ex] .
4. S. X. Nakamura, A. Hosaka, and Y. Yamaguchi, Phys. Rev. D **104**, L091503 (2021), arXiv:2109.15235 [hep-ph] .
5. J. Ferretti and E. Santopinto, (2021), arXiv:2111.08650 [hep-ph] .
6. M. I. Eides, V. Y. Petrov, and M. V. Polyakov, Phys. Rev. D **93**, 054039 (2016), arXiv:1512.00426 [hep-ph] .
7. M. I. Eides, V. Y. Petrov, and M. V. Polyakov, Eur. Phys. J. C **78**, 36 (2018), arXiv:1709.09523 [hep-ph] .
8. M. I. Eides, V. Y. Petrov, and M. V. Polyakov, Mod. Phys. Lett. A **35**, 2050151 (2020), arXiv:1904.11616 [hep-ph] .
9. X.-K. Dong, V. Baru, F.-K. Guo, C. Hanhart, and A. Nefediev, Phys. Rev. Lett. **126**, 132001 (2021), arXiv:2009.07795 [hep-ph] .
10. X.-K. Dong, V. Baru, F.-K. Guo, C. Hanhart, A. Nefediev, and B.-S. Zou, Sci. Bull. **66**, 2462 (2021), arXiv:2107.03946 [hep-ph] .
11. J. Ferretti and E. Santopinto, JHEP **04**, 119 (2020), arXiv:2001.01067 [hep-ph] .
12. M.-Z. Liu, F.-Z. Peng, M. Sánchez Sánchez, and M. P. Valderrama, Phys. Rev. **D98**, 114030 (2018), arXiv:1811.03992 [hep-ph] .
13. M.-Z. Liu, Y.-W. Pan, F.-Z. Peng, M. Sánchez Sánchez, L.-S. Geng, A. Hosaka, and M. Pavon Valderrama, Phys. Rev. Lett. **122**, 242001 (2019), arXiv:1903.11560 [hep-ph] .
14. C. Xiao, J. Nieves, and E. Oset, Phys. Rev. D **100**, 014021 (2019), arXiv:1904.01296 [hep-ph] .
15. M. Pavon Valderrama, Phys. Rev. **D100**, 094028 (2019), arXiv:1907.05294 [hep-ph] .
16. M.-Z. Liu, T.-W. Wu, M. Sánchez Sánchez, M. P. Valderrama, L.-S. Geng, and J.-J. Xie, Phys. Rev. D **103**, 054004 (2021), arXiv:1907.06093 [hep-ph] .
17. F.-K. Guo, H.-J. Jing, U.-G. Meißner, and S. Sakai, Phys. Rev. **D99**, 091501 (2019), arXiv:1903.11503 [hep-ph] .
18. M.-L. Du, V. Baru, F.-K. Guo, C. Hanhart, U.-G. Meißner, J. A. Oller, and Q. Wang, Phys. Rev. Lett. **124**, 072001 (2020), arXiv:1910.11846 [hep-ph] .
19. M.-L. Du, V. Baru, F.-K. Guo, C. Hanhart, U.-G. Meißner, J. A. Oller, and Q. Wang, JHEP **08**, 157 (2021), arXiv:2102.07159 [hep-ph] .
20. Y. Yamaguchi, H. García-Tecocoatzi, A. Giachino, A. Hosaka, E. Santopinto, S. Takeuchi, and M. Takizawa, Phys. Rev. D **101**, 091502 (2020), arXiv:1907.04684 [hep-ph] .
21. B. Wang, L. Meng, and S.-L. Zhu, JHEP **11**, 108 (2019), arXiv:1909.13054 [hep-ph] .
22. T. J. Burns, Eur. Phys. J. **A51**, 152 (2015), arXiv:1509.02460 [hep-ph] .
23. L. Geng, J. Lu, and M. P. Valderrama, Phys. Rev. **D97**, 094036 (2018), arXiv:1704.06123 [hep-ph] .
24. T. J. Burns and E. S. Swanson, Phys. Rev. D **100**, 114033 (2019), arXiv:1908.03528 [hep-ph] .
25. F.-Z. Peng, J.-X. Lu, M. Sánchez Sánchez, M.-J. Yan, and M. Pavon Valderrama, Phys. Rev. D **103**, 014023 (2021), arXiv:2007.01198 [hep-ph] .
26. E. Ortiz-Pacheco, R. Bijker, and C. Fernández-Ramírez, J. Phys. G **46**, 065104 (2019), arXiv:1808.10512 [nucl-th] .
27. Z.-G. Wang, Int. J. Mod. Phys. A **35**, 2050003 (2020), arXiv:1905.02892 [hep-ph] .
28. S.-Q. Kuang, L.-Y. Dai, X.-W. Kang, and D.-L. Yao, Eur. Phys. J. C **80**, 433 (2020), arXiv:2002.11959 [hep-ph] .
29. M. Albaladejo, F.-K. Guo, C. Hidalgo-Duque, and J. Nieves, Phys. Lett. B **755**, 337 (2016), arXiv:1512.03638 [hep-ph] .
30. Z. Yang, X. Cao, F.-K. Guo, J. Nieves, and M. P. Valderrama, Phys. Rev. D **103**, 074029 (2021), arXiv:2011.08725 [hep-ph] .
31. C. Fernández-Ramírez, A. Pilloni, M. Albaladejo, A. Jackura, V. Mathieu, M. Mikhasenko, J. A. Silva-Castro, and A. P. Szczepaniak (JPAC), Phys. Rev. Lett. **123**, 092001 (2019), arXiv:1904.10021 [hep-ph] .
32. R. Chen, A. Hosaka, and X. Liu, Phys. Rev. D **96**, 116012 (2017), arXiv:1707.08306 [hep-ph] .
33. C.-W. Shen, D. Rönchen, U.-G. Meißner, and B.-S. Zou, Chin. Phys. C **42**, 023106 (2018), arXiv:1710.03885 [hep-ph] .
34. J. He and D.-Y. Chen, Eur. Phys. J. C **79**, 887 (2019), arXiv:1909.05681 [hep-ph] .
35. H.-W. Ke, M. Li, X.-H. Liu, and X.-Q. Li, Phys. Rev. D **101**, 014024 (2020), arXiv:1909.12509 [hep-ph] .
36. H.-X. Chen, W. Chen, X. Liu, and X.-H. Liu, Eur. Phys. J. C **81**, 409 (2021), arXiv:2011.01079 [hep-ph] .
37. M.-Z. Liu, Y.-W. Pan, and L.-S. Geng, Phys. Rev. D **103**, 034003 (2021), arXiv:2011.07935 [hep-ph] .
38. F.-Z. Peng, M.-J. Yan, M. Sánchez Sánchez, and M. P. Valderrama, Eur. Phys. J. C **81**, 666 (2021), arXiv:2011.01915 [hep-ph] .
39. X.-K. Dong, F.-K. Guo, and B.-S. Zou, Progr. Phys. **41**, 65 (2021), arXiv:2101.01021 [hep-ph] .
40. C. W. Xiao, J. Nieves, and E. Oset, Phys. Lett. B **799**, 135051 (2019), arXiv:1906.09010 [hep-ph] .
41. B. Wang, L. Meng, and S.-L. Zhu, Phys. Rev. D **101**, 034018 (2020), arXiv:1912.12592 [hep-ph] .

42. D. B. Kaplan, M. J. Savage, and M. B. Wise, Phys. Lett. **B424**, 390 (1998), arXiv:nucl-th/9801034 .
43. D. B. Kaplan, M. J. Savage, and M. B. Wise, Nucl. Phys. **B534**, 329 (1998), arXiv:nucl-th/9802075 .
44. S. Fleming, T. Mehen, and I. W. Stewart, Nucl. Phys. **A677**, 313 (2000), arXiv:nucl-th/9911001 [nucl-th] .
45. U. van Kolck, Nucl. Phys. A **645**, 273 (1999), arXiv:nucl-th/9808007 .
46. M. Pavón Valderrama, M. Sánchez Sánchez, C. J. Yang, B. Long, J. Carbonell, and U. van Kolck, Phys. Rev. C **95**, 054001 (2017), arXiv:1611.10175 [nucl-th] .
47. M. P. Valderrama, Phys. Rev. **D85**, 114037 (2012), arXiv:1204.2400 [hep-ph] .
48. C. Hanhart, J. R. Pelaez, and G. Rios, Phys. Lett. B **739**, 375 (2014), arXiv:1407.7452 [hep-ph] .
49. S. Ahmed *et al.* (CLEO Collaboration), Phys. Rev.Lett. **87**, 251801 (2001), arXiv:hep-ex/0108013 [hep-ex] .
50. A. Anastassov *et al.* (CLEO Collaboration), Phys. Rev. **D65**, 032003 (2002), arXiv:hep-ex/0108043 [hep-ex] .
51. P. Zyla *et al.* (Particle Data Group), PTEP **2020**, 083C01 (2020).
52. T. Mehen, Phys. Rev. D **92**, 034019 (2015), arXiv:1503.02719 [hep-ph] .
53. M.-J. Yan and M. P. Valderrama, Phys. Rev. D **105**, 014007 (2022), arXiv:2108.04785 [hep-ph] .
54. H.-Y. Cheng and C.-K. Chua, Phys. Rev. **D92**, 074014 (2015), arXiv:1508.05653 [hep-ph] .
55. P. L. Cho, Nucl. Phys. **B396**, 183 (1993), [Erratum: Nucl. Phys. **B421**, 683(1994)], arXiv:hep-ph/9208244 [hep-ph] .
56. T.-M. Yan, H.-Y. Cheng, C.-Y. Cheung, G.-L. Lin, Y. C. Lin, and H.-L. Yu, Phys. Rev. **D46**, 1148 (1992), [Erratum: Phys. Rev. **D55**, 5851(1997)].
57. J.-X. Lu, L.-S. Geng, and M. P. Valderrama, Phys. Rev. **D99**, 074026 (2019), arXiv:1706.02588 [hep-ph] .
58. S. R. Beane, P. F. Bedaque, L. Childress, A. Kryjevski, J. McGuire, and U. van Kolck, Phys. Rev. A **64**, 042103 (2001), arXiv:quant-ph/0010073 .
59. T. Barford and M. C. Birse, Phys. Rev. **C67**, 064006 (2003), arXiv:hep-ph/0206146 [hep-ph] .
60. A. Nogga, R. G. E. Timmermans, and U. van Kolck, Phys. Rev. C **72**, 054006 (2005), arXiv:nucl-th/0506005 .
61. M. Pavon Valderrama and E. R. Arriola, Phys. Rev. **C74**, 054001 (2006), arXiv:nucl-th/0506047 .
62. M. Pavon Valderrama and E. Ruiz Arriola, Phys. Rev. **C74**, 064004 (2006), arXiv:nucl-th/0507075 .
63. M. C. Birse, Phys. Rev. **C74**, 014003 (2006), arXiv:nucl-th/0507077 [nucl-th] .
64. A. Ali *et al.* (GlueX), Phys. Rev. Lett. **123**, 072001 (2019), arXiv:1905.10811 [nucl-ex] .
65. T. J. Burns and E. S. Swanson, Eur. Phys. J. A **58**, 68 (2022), arXiv:2112.11527 [hep-ph] .
66. F.-Z. Peng, M.-Z. Liu, M. Sánchez Sánchez, and M. Pavon Valderrama, Phys. Rev. D **102**, 114020 (2020), arXiv:2004.05658 [hep-ph] .
67. F.-Z. Peng, M. Sánchez Sánchez, M.-J. Yan, and M. Pavon Valderrama, Phys. Rev. D **105**, 034028 (2022), arXiv:2101.07213 [hep-ph] .
68. S. Sakai, H.-J. Jing, and F.-K. Guo, Phys. Rev. D **100**, 074007 (2019), arXiv:1907.03414 [hep-ph] .
69. F.-Z. Peng, M.-Z. Liu, Y.-W. Pan, M. Sánchez Sánchez, and M. Pavon Valderrama, (2019), arXiv:1907.05322 [hep-ph] .
70. C. W. Xiao, J. Nieves, and E. Oset, Phys. Rev. D **88**, 056012 (2013), arXiv:1304.5368 [hep-ph] .
71. M. C. Birse, J. A. McGovern, and K. G. Richardson, Phys. Lett. **B464**, 169 (1999), arXiv:hep-ph/9807302 [hep-ph] .
72. M. Pavón Valderrama and D. R. Phillips, Phys. Rev. Lett. **114**, 082502 (2015), arXiv:1407.0437 [nucl-th] .
73. M. P. Valderrama, Int. J. Mod. Phys. **E25**, 1641007 (2016), arXiv:1604.01332 [nucl-th] .
74. E. Epelbaum, J. Gegelia, and U.-G. Meißner, Nucl. Phys. B **925**, 161 (2017), arXiv:1705.02524 [nucl-th] .
75. J.-W. Chen, G. Rupak, and M. J. Savage, Nucl. Phys. A **653**, 386 (1999), arXiv:nucl-th/9902056 .